2014

A Sustainable Industrial Waste Management Solution: Application Of Silica Fume To Enhance Asphalt Binder Rheological Properties

Nader T. Abutalib
North Carolina Agricultural and Technical State University

A Sustainable Industrial Waste Management Solution:

Application of Silica Fume to Enhance Asphalt Binder Rheological Properties

Nader T. Abutalib

North Carolina A&T State University

A thesis submitted to the graduate faculty

in partial fulfillment of the requirements for the degree of

MASTER OF SCIENCE

Department: Civil, Architectural and Environmental Engineering Department

Major: Civil Engineering

Major Professor: Dr. Ellie Fini

Greensboro, North Carolina

2014

The Graduate School
North Carolina Agricultural and Technical State University
This is to certify that the Master's Thesis of

Nader T. Abutalib

has met the thesis requirements of
North Carolina Agricultural and Technical State University

Greensboro, North Carolina
2014

Approved by:

Dr. Ellie Fini Major Professor	Dr. Sameer Hamoush Committee Member
Dr. Taher Abu Lebdeh Committee Member	Dr. Sameer Hamoush Department Chair

Dr. Sanjiv Sarin
Dean, The Graduate School

Biographical Sketch

Nader T. Abutalib was born on Sep 26, 1985, in the city of Makkah in Saudi Arabia. His love of engineering was discovered when he was in high school. While gaining basic knowledge in engineering, he also excelled as a computer programmer. This combination allowed him to continue his studies both in Saudi Arabia and abroad. In 2003, he was accepted in the civil engineering specialization as an undergraduate student in Umm Al-Qurra University in Makkah. In addition, he traveled overseas during summer sessions for computer programmer training on programs such as AutoCAD and geographic information systems (GIS). With undergraduate courses as his base and relevant knowledge in the field of civil engineering, he represented his university in national competitions in Saudi Arabia. Abutalib completed his undergraduate studies in 2008, earning a Bachelor's of Science degree in civil engineering.

In 2008, he had the opportunity to work in the Ministry of Municipal Affairs as a civil engineer in his town. This experience created a passion in him to gain the knowledge and credentials to work in this field. He worked in a variety of departments to provide public services to the community, gaining experience with different methods of supporting the city infrastructure.

In 2010, he realized that he has many traits and interests that would make him an appropriate candidate for graduate studies. In order to continue his studies, he had to satisfy the requirement for English proficiency. He earned a diploma of academic English from the Interlink Language Center at UNC Greensboro.

With his initial interest in transportation engineering, he chose to continue his studies as a graduate student in the Department of Civil Engineering at North Carolina A&T State University. He was eager to become well-read in the area of transportation engineering and do

his own research. Abutalib focused his research and studies on the inclusion of nano-particles in asphalt binder to improve the rheological properties and aging susceptibility of asphalt. During this study, he had the opportunity to attend appropriate classes to be able to cover the concept and be well-prepared to achieve the target of his research.

Dedication

I would like to dedicate this thesis with my warm appreciation to my family: my father, Mr. Turki Abutalib; my mother, Mrs. Zain Alsulimani; my wife, Mrs. Yosra Alsulimani; and my brother, Mr. Mohammad Abutalib. The hard work that went into this thesis is a result of the characteristics that have been instilled in me by my family, and I thank them for being with me through the struggles that I faced.

I want to especially thank my mother, who encouraged me to achieve my goal and supported me without hesitation in circumstances that were beyond her control. This dedication is in appreciation to my mother, Mrs. Zain Alsulimani, with love.

Acknowledgements

I would like to thank my advisor, Dr. Ellie Fini, who significantly prepared me to achieve my goal. After she carefully reviewed my experience and looked at my sense of engineering, she helped me to improve my knowledge and guided me to the appropriate classes to a great thought of sustainable pavements. I would also like to thank Daniel Oldham and Albert Onochie, who are members of Dr. Fini's research team. They were knowledgeable on the topic and they did not hesitate to help when I was asking. I would also like to acknowledge the valuable help from Renaldo Walters, who helped with conducting my XRD and FTIR tests and analysis.

Table of Contents

List of Figures

List of Tables

Abstract

This thesis investigates the practical feasibility of using silica fume, an industrial waste material, to enhance the rheological properties of asphalt binder. It has been widely reported that asphalt binder oxidation reduces the service life of asphalt pavement by negatively impacting its rheological properties. When asphalt binder is oxidized, its viscoelastic properties are diminished; this can be evidenced by the reduction in asphalt phase angle as measured through dynamic shear and torsion tests. This can lead to a more brittle pavement, which is more prone to cracks due to thermal stress and traffic loading and leads to premature pavement failure. In this thesis, the effectiveness of the application of silica-fume-based additives to reduce asphalt oxidative aging is investigated. It is hypothesized that fine-graded silica fume with nano- to micro-level particle size can be used to reduce asphalt oxidation. To test this hypothesis, various percentages of silica fume were introduced to base binders; then a series of experiments in binder and mixture level was conducted to evaluate the effects of silica fume addition. In the binder level, silica fume was concentrated in asphalt binder with percentages of 2%, 4%, and 8% for both aged and non-aged samples. A rotational viscometer (RV) was used to study the effects of silica fume on high-temperature properties of asphalt binder. FTIR analysis was used to determine the chemical compounds of silica-fume-modified asphalt matrix. The Marshall stability test was used to evaluate the stability of the asphalt mixture in the presence of silica fume. Analysis of the experiment results showed that silica fume reduced the asphalt aging index significantly; in addition, the temperature susceptibility of asphalt binder was reduced as the percentage of silica fume increased. The positive effect of silica fume on base asphalt's rheological properties could be attributed to the high surface area of the silica fume accompanied by its granular particles with high polarity.

CHAPTER 1

Introduction

It has been well reported that asphalt aging is mainly associated with oxidation at the molecular level. The increased oxidation has been shown to decrease the service life of roads. When asphalt binder is oxidized, its viscoelastic properties are diminished; this can be evidenced by the reduction in asphalt phase angle as measured through dynamic shear and torsion tests. This in turn can lead to a more brittle pavement, which is more prone to cracks due to thermal stress and traffic loading and leads to premature pavement failure. This phenomenon is known to be expedited at high temperature, accompanied by loss of asphalt volatile compounds. Oxidation affects molecular chains in the pavement, leading to their breakdown as well as creating new chemical compounds, including carbonyl and sulfoxide compounds that are naturally present in asphalt binder. These in turn lead to an increase in asphalt binder viscosity while reducing its phase angle as the oxidation progresses. This results in a stiffer and more brittle material (Huang et al., 2012). In this thesis, the effectiveness of the application of silica-fume-based additives to reduce asphalt oxidative aging is investigated. It is hypothesized that fine-graded silica fume with nano- to micro-level particle size can be used to reduce asphalt oxidation, creating a new generation of asphalt pavement with higher resistance to oxidative aging.

Polymers have a variety of applications that have led researchers to investigate polymers to address many of today's problems. High temperature causes erosion and decays most man-made structures, including roads. The presence of water weakens the molecular bonds between asphalt and its aggregate parts. Moisture leads to breakdown of the molecular chains in the pavement, causing holes and the need for repaving (Yildirim, 2007). Repaving costs money and

time, and increases the amount of VOCs (volatile organic compounds) that are released into the atmosphere.

Nano-silica has been highly used in the polymer industry to increase mechanical and physical properties of base materials such as stiffness, toughness, strength, and thermal stability (Lee et al., 2005). Recently, there have been studies on the use of various nano-particles to modify asphalt binders; for instance, it has been shown that nano-clay can be an effective additive for use in asphalt binder (Onochie et al., 2013). Furthermore, studies reported that the presence of layered silicate montmorillonite (MMT) nano-clay in asphalt binder can significantly reduce asphalt oxidative aging, provided that intercalation or exfoliation of silicate layers can be achieved. Typically, intercalation or exfoliation has been facilitated using nano-clay modification. A modification that has been reported effective in facilitating exfoliation of silicate layers has been organo-modification of clay particles (Yu et al., 2010). The level of exfoliation has been monitored mainly by measuring the spacing of silicate layers using X-ray diffraction.

Other studies have used nano-silica to achieve a highly polar surface and reported that nano-silica can be very effective in reducing the aging rate while enhancing resistance to rutting and cracking (Amerkhanian et al., 2010). In fact, modifiers such as silica fume have the capability to enhance the aging resistance of asphalt binder as well as extend the asphalt's high- and low-temperature workability. However, to achieve such improvements, it is critical to ensure uniform blending of nano-silica into the asphalt matrix. Agglomeration of nano-silica particles has been reported to be an issue for such applications. Therefore, this study investigates the effectiveness of silica fume in the form of a granulated industrial waste with highly polar surface area to enhance blending and improve asphalt oxidation resistance.

It has been reported that approximately 5.11 million tons of silica fume were produced in 2010, and 4.78 million tons in 2012. Since silica fume is a frequently available industrial waste (Haipeng, 2014), its application in asphalt paving could facilitate industrial waste management while improving asphalt sustainability and performance. Silica fume is a very fine pozzolanic material with an average particle size of 100 – 200 nm. It is extracted from gases produced while making silicon or ferrosilicon alloy at 1750°C. The exhaust dust from the smoke is then collected on electrostatic filters as silica fume (SFA, 2005). Silica fume is made of extremely fine granulated particles that have very high silica content. Its surface area ranges from 60,000 to 150,000ft^2/lb, and it has a specific gravity of 2.20. Silica fume is categorized as nano-particles because of the size ranges and particle shape. Due to its polarity and high surface area, it can be used as an additive in asphalt binder to improve the properties of the asphalt binder (Markovic and Mikoc, 2010).

This thesis focuses on using silica fume as an additive to enhance the rheological properties of asphalt binder. Using penetration grade 60-70 asphalt binder, five asphalt mixtures were made containing silica fume: 0.25%, 0.5%, and 1% silica fume were incorporated. These modified mixtures were tested along with a control sample (without silica fume) to determine the stability and flow. In the binder level, the base asphalt binder PG 64-22, which is commonly used in North Carolina, was used for the study. Modified specimens were made by incorporating 2%, 4%, and 8% of silica fume into the aforementioned base asphalt. Modified and non-modified asphalt binders were compared in terms of their viscosity, shear, and temperature susceptibility before and after being exposed to oxidative aging. Figure 1-1 shows the experiment plan of this study, with a total of 12 samples: 4 samples were used in the mixture level, and 8 samples were used in the binder level.

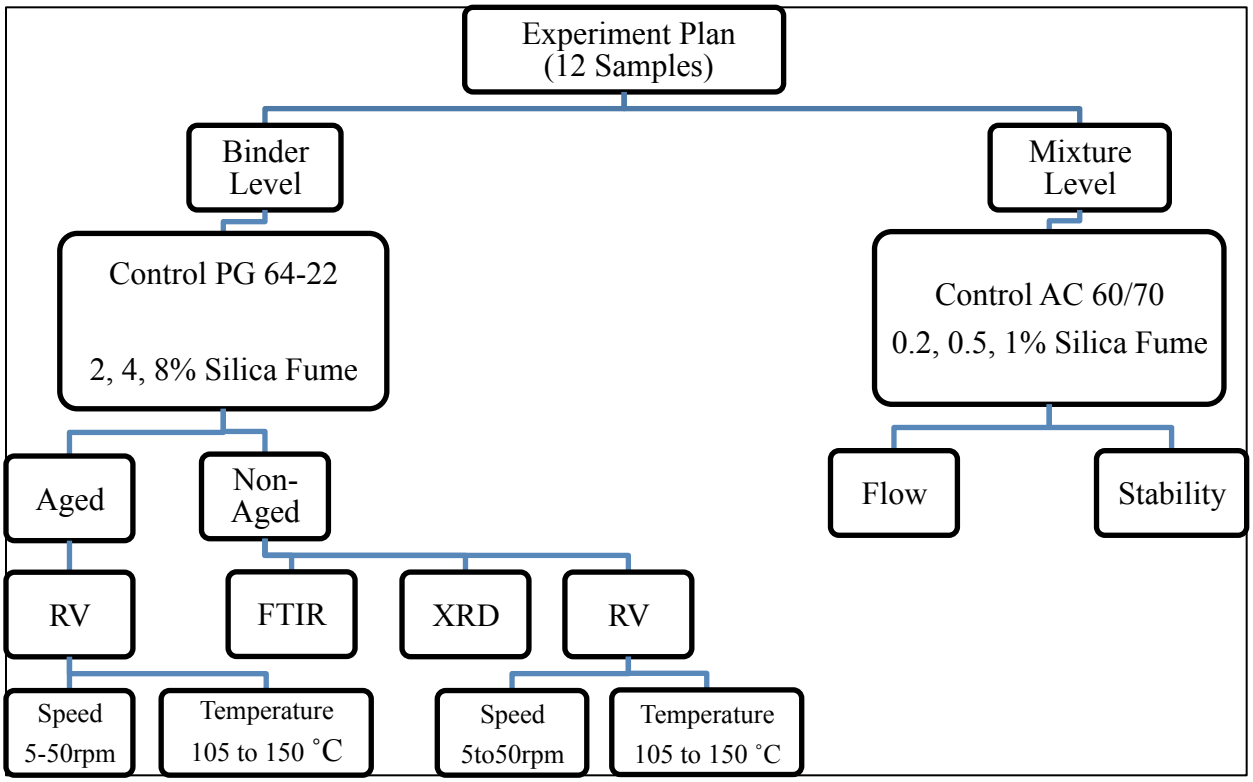

Figure 1-1. Experiment Plan

1.1 Background

1.1.1 Asphalt binder (PG 64-22)

This advanced bitumen is used in paving for new construction and pavement rehabilitation. The heating temperature of the bitumen is 177˚C. Its flash point is 325˚C. The storage temperature range is 140˚C to 168˚C. Increases in temperature cause increased hardening, oxidation, and heating cost. (U.S. Oil & Refining Co.). Typical physical properties of asphalt binder are shown in Table 1-1.

Table 1-1

Typical Physical Properties of Asphalt Binder (ASTM International, 2013)

Property	Test Method	Value
Flash Point, °C Cleveland Open Cup	ASTM D92, EN 22592 (b)	Varies according to grade, Typically > 230°C (445°F). > 270°C (520°F) in ASTM D312, > 250°C (482°F) in EN 13304
Loss on Heating, % m (Maximum)	ASTM D2872, EN 12607-1	0.5-1% maximum depending upon the specification
Specific gravity value	ASTM D70 EN 15326	≥ 0.95, typically > 1.0, not a specification
Solubility, % (Minimum)	ASTM D2042, EN 12592	≥ 0.99% m by specification (Trichloroethylene, Toluene, or Xylene as specified)
Solubility in water		Negligible
Softening Point	ASTM D86, EN 1427	> 30°C (86°F, grade dependent
Vapor Pressure		Below detection limit at ambient temperature

1.1.1.1 Components of asphalt pavement materials

Asphalt is made of bitumen or modified polymer bituminous binder, additives such as bonding and stripping agents, and air. Other particles such as fibers, crumb rubber, glass, slag, or silica fume could be added to asphalt to reduce the risk of rutting, low temperature cracking, and fatigue cracking (You et al., 2011), (Yu et al., 2010).

1.1.2 Silica fume

Silica fume is extremely fine non-crystalline silica that is produced in electric arc furnaces as a by-product of elemental silicon production. Figure 1-1 is a photograph that shows

the color of silica fume. It shows typical silica fume as it is collected from a furnace. Usually, silica fume is a powder that has a gray color. Silica fume is extracted from silicon metal. Using the desired reaction $SiO2 + 2C = Si + 2CO$, the smoke that results from raw materials quartz, coal, and woodchips is silica fume. Figure 1-3 and Figure 1-4 are schematics of a smelter for silicon metal production that show how silica fume is produced. Silica fume is collected in the baghouse (SFA, 2005). Silica fume is considered an industrial waste that is commonly available. Approximately 5.11 million tons of silica fume were produced in 2010, and 4.78 million tons in 2012 (Haipeng et al., 2014). One of the highest uses of silica fume is as an additive to concrete. Silica fume has significant chemical and physical properties that make it a reactive pozzolan. Adding silica fume to concrete results in high strength and considerable improvement in concrete properties (SFA, 2005).

Figure 1-2. Silica Fume

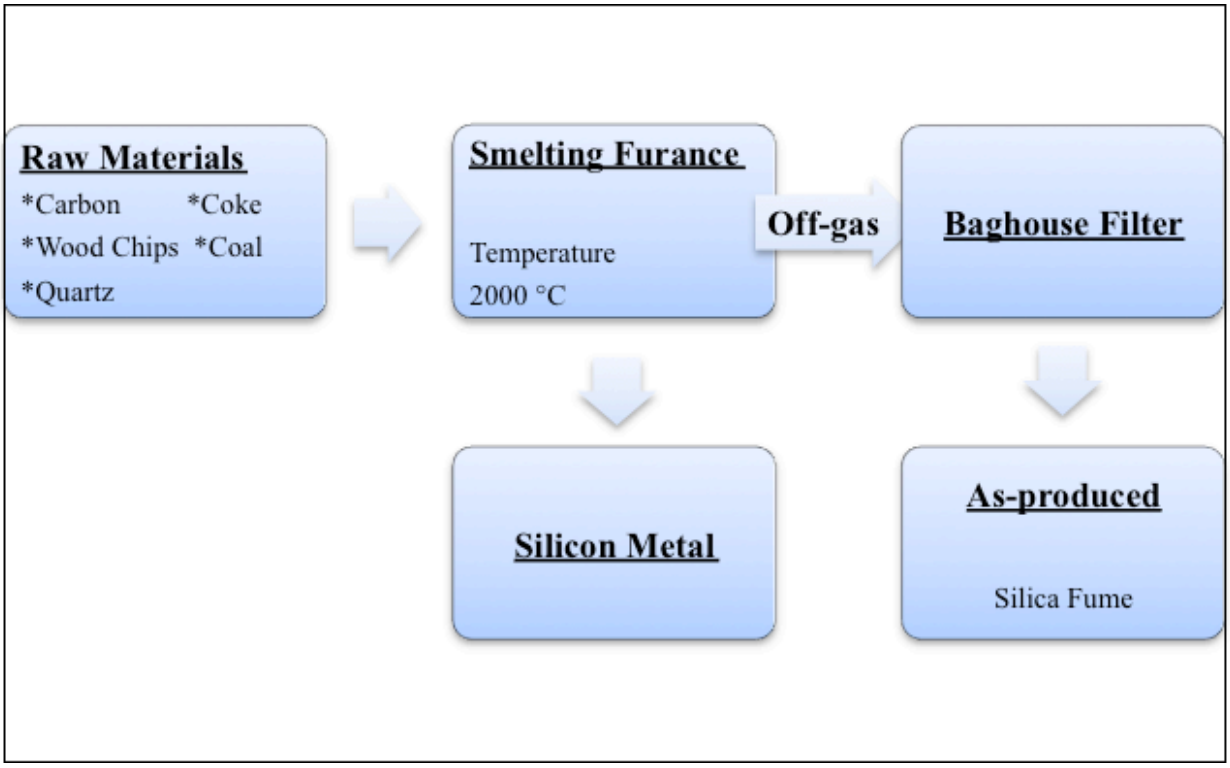

Figure 1-3. Silica Fume Production

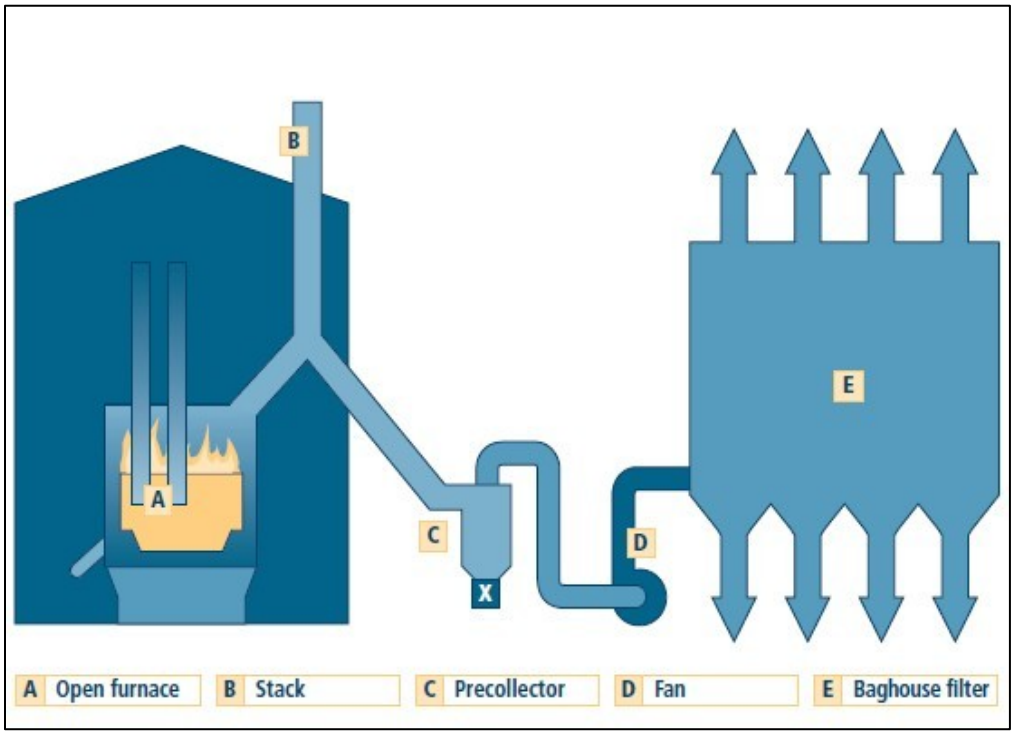

Figure 1-4. Silica Fume Production (SFA, 2005)

1.1.2.1 Chemical properties of silica fume

Silica fume is amorphous and may contain other elements. Following is a discussion of each of these properties (SFA, 2005).

Amorphous

Silica fume is a non-crystalline material. In fact, a crystalline material is not dissolvable in concrete, which should occur before the material can react with the concrete. Sand is a crystalline material in concrete that is chemically similar to silica fume. Essentially, sand is silicon dioxide (SiO_2). Therefore, because of its crystalline nature, sand does not react.

Trace elements

There may be additional materials in silica fume, based on the metal being produced in the smelter from which the fume was recovered. Usually, these materials have no impact on the silica fume's performance in concrete. Standard specifications for silica fume require that it contain less than 85% silicon dioxide.

1.1.2.2 Physical properties of silica fume

Below is a discussion of four physical properties of silica fume.

Particle size

Silica fume has extremely small particles. Most of the particles are less than 1 μm in size. Particle size has significant effects on the physical and chemical contributions of silica fume in concrete. Figure 1-5 shows a photomicrograph of Portland cement grains. The silica-fume

particles at the same magnification are shown in Figure 1-6. The longer white line in Figure 1-6 is one micrometer long. In a 15% silica-fume addition by weight to cement, there are approximately 2,000,000 particles of silica fume for each grain of Portland cement (SFA, 2005).

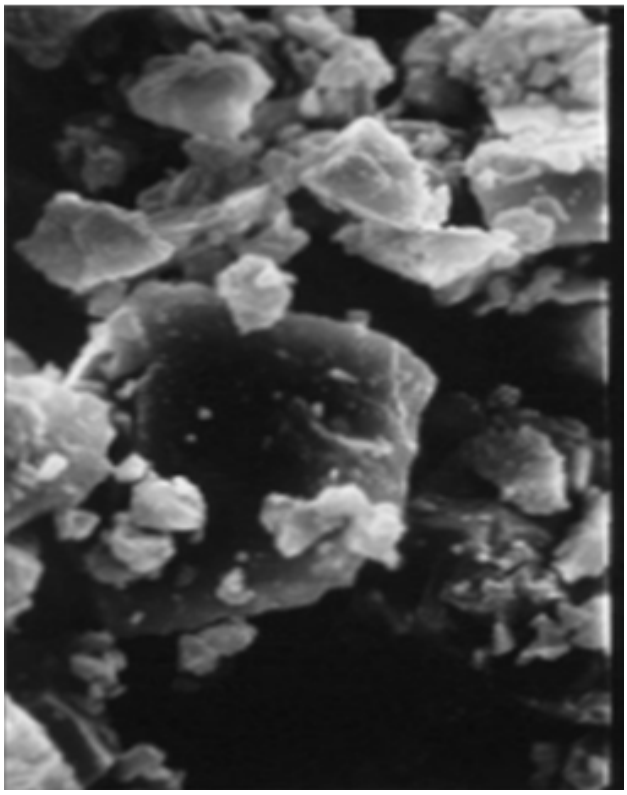

Figure 1-5. A Photograph of Portland Cement Grains (SFA, 2005)

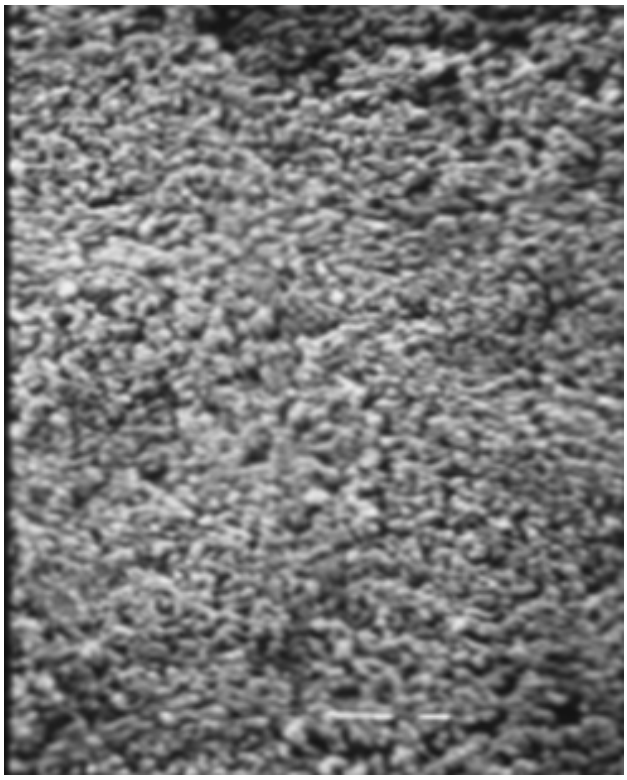

Figure 1-6. A Photograph of Silica Fume Particles (SFA, 2005)

Bulk density

Bulk density is a term for unit weight. The produced fume bulk density depends on the metal that made in the furnace. The silica fume as-produced bulk density range is 130 to 430 kg/m^3, while the density range of the densified fume is 480 to 720 kg/m^3. The bulk density of as-produced silica fume is low. Therefore, it is hard to transport it for long distances (SFA, 2005).

Specific gravity

Specific gravity is a term that relates the compression of silica fume to that of water, which has a specific gravity of 1.00. Silica fume has a specific gravity of 2.2. In fact, Portland cement has a specific gravity of 3.15. So silica fume is lighter than Portland cement. Thus, adding silica fume to a concrete mixture will not densify the concrete (SFA, 2005).

Surface area

Surface area of a material mass gives the result of specific surface. Silica fume particles are extremely small. Therefore, silica fume has a high surface area of 15,000 to 30,000 m^2/kg. In fact, water demand increases for sand as the particles become smaller, the same as for silica fume. Thus, it is necessary to use silica fume in combination with a water-reducing admixture. The Silica Fume Association indicated that a "specialized test called the "BET method" or "nitrogen adsorption method" must be used to measure the specific surface of silica fume. Specific surface determinations based on sieve analysis or air-permeability testing are meaningless for silica fume".

1.1.2.3 Standard specifications for silica fume

There are two standard specifications for silica fume: ASTM-C-1240, which is the Standard Specification for Silica Fume Used in Cementitious Mixtures; and AASHTO-M-307, which is the Standard Specification for Use of Silica Fume as a Mineral Admixture in Hydraulic-Cement Concrete, Mortar, and Grout.

Each of these specifications contains both mandatory and optional elements. The ASTM-C-1240 and AASHTO-M-307 specifications were derived from other pozzolan specifications such as ASTM-C-618, Standard Specification for Raw Natural Pozzolan and Coal Fly Ash for Use in Concrete. The Silica Fume Association has shown that "because of this origin, some of the requirements for silica fume are actually more appropriate for other pozzolanic materials. Over time these elements of the specifications are being revised or removed."

1.2 Objectives

The research study in this thesis focuses on evaluating the effects of adding different percentages of silica fume on the rheological properties and aging susceptibility of asphalt binder:

- Determine the viscosity of silica-fume-modified asphalt binder when 2%, 4%, and 8% (weight of dry mass) silica fume are added to virgin asphalt binder (PG 64-22).
- Determine the flow and loss of stability of silica-fume-modified asphalt mixture when 0.25%, 0.5%, and 1% (weight of dry mass) silica fume are added to asphalt (60-70).
- Determine the crystalline structure of the silica-fume-modified binder.
- Determine the chemical bonds in the silica-fume-modified binder.

1.3 Research Approach

The hypothesis of this research is that the inclusion of silica fume in asphalt binder enhances asphalt binder's rheological properties and reduces its aging susceptibility. To test this hypothesis, the following research approach was considered to evaluate the rheological characteristics and chemical bonds in control asphalts and asphalts modified with three selected percentages of silica fume:

· Rotational Viscosity (RV) test

RV is the abbreviation for rotational viscometer. The RV test was conducted according to the ASTM D4402 standard specification using the Brookfield rotational viscometer. Tests were conducted at 120°C, 135°C, and 150°C. In this study, test results were used to compare dynamic shear viscosity among the asphalt modifications.

· X-Ray Diffraction test

This test was conducted using a diffractometer system. This test is used to characterize polycrystalline structure of materials. The powder diffraction identifies components in a sample by procedure matching. In this study, test results were used to determine the crystallography of the tested mixtures. Data was collected between the angles of 4 and 60

2Theta for a period of two hours for each sample. For silica fume samples, 0.04 RAD soller slits were used, which increase the intensity of the X-Ray beam. The soller slit job is to take a line source of radiation and distribute it into smaller beams, leading to reduced axial divergence of the beam.

· Fourier Transform Infrared (FTIR) spectroscopy test

FTIR was used to determine the unknown chemical bonds of silica fume that have occurred due to the synthesis of material. This test was conducted at room temperature for all samples. This test can be used to determine the stability of a substance.

1.4 Research Scope

Chapter 1 describes the purpose of the research, the study objectives, and the hypothesis. Chapter 2 contains a literature review. Chapter 3 describes the preliminary study to investigate the workability of adding silica fume to an asphalt mixture. In Chapter 4, the approaches have been tested to measure rheological characteristics of modified and non-modified asphalt in the binder level. It also presents the material properties of silica fume. Chapter 5 discusses the test procedures and results from each of the tests that have been mentioned. Chapter 6 contains discussion and conclusions of the research.

CHAPTER 2

Literature Review

There have been many studies on investigating asphalt binder oxidation mechanisms; many researchers tried to develop modifiers and additives to enhance asphalt binder's resistance to oxidative aging. Oxidative aging of asphalt binder is expedited when heated at the application temperature and mixed with stone aggregates; this usually is accompanied by significant loss of volatile compounds, while giving rise to carbonyl and sulfoxide compounds in asphalt (Lu and Isacsson, 2002).

Asphalt binder properties could be negatively affected by oxidative aging, diminishing the binder's rheological properties and leading to premature pavement cracking. Therefore, it is important to reduce the level of asphalt oxidation during both asphalt application and pavement service life. Asphalt is one of the main components used in highway and airport pavements; more than 90% of roads in the U.S. are made of asphalt pavement, and the rest are concrete. Worldwide annual consumption of asphalt in 2013 was 150 million tons, making it an 80 billion dollar industry. In the U.S., generally 90% of liquid asphalt is used for road paving and approximately 10% is used for roofing products, with other specialty applications accounting for only a very small fraction of consumption (SBI, 2009).

Using polymers for asphalt binder modification has become the standard in ideal pavement design, especially in the United States, Canada, Europe, and Australia. There are many polymers, such as rubber, SBR, SBS, and Elvaloy that have been used in the specifications designed to modify binders. The elastic recovery test provides valuable results once polymers are present in an asphalt binder (Yildirim, 2007). Asphalt has been studied by many associations and researchers looking for the best way to resist rainfall and ground water impacts, and improve

asphalt properties for high quality pavement. It is crucial to play a proactive role in maintaining pavement by preventing problems before they start. From day one, as soon as asphalt pavement is installed, numerous factors are working to deteriorate the pavement surfaces. Asphalt begins aging the minute it is laid, as oxidation causes the oil in the binder to evaporate. At first, this is good, because it allows the asphalt to cure. Eventually, though, the pavement gets too dry, leading to raveling and hairline cracks. Before these cracks begin to develop, or while they are still small, an asphalt seal coat should be applied by a professional seal coat contractor. Asphalt is the term used to describe a mixture of bitumen (oil) with aggregate (rock) (Parviz, 2011). Asphalt may also contain other additives such as emulsifiers, cutback agents, polymers, etc. Asphalt pavement is this mixture placed and compacted over a base course or a sub base course, or both. This pavement is also referred to as a pavement structure in that each course (surface, base, sub-base) will act structurally and each provides support to the given loading.

Considering liquid asphalt's wide applications mainly for outdoor applications and in various environmental conditions, developing techniques and methodology to reduce the rate of asphalt oxidative aging is critical. New efforts and studies of materials engineered at the nano-scale in other engineering fields may well lead to major improvements in the mechanical and physical properties as well as the durability of composite construction materials. Application of such technology in the field of asphalt in order to address issues such as oxidation has received significant attention recently. Thus, many researchers investigated various nano-particles as modifiers to prevent oxidative aging; among those, nano-clay and nano-silica were found to be effective in reducing the asphalt aging index (Onochie et al., 2013). This thesis investigates the merits of application of very fine granulated silica particles (100nm - 200nm) to reduce oxidative aging of asphalt binder.

The effects of using silica fume in cementitious products such as concrete, grouts, and mortars as well as elastomer, polymer, refractory, ceramic, and rubber applications has been well documented (Khayat et al., 1997). In cementitious compounds, silica fume initiates a chemical reaction called the pozzolanic reaction. The hydration of Portland cement produces compounds such as calcium silicate hydrates (CSH) and calcium hydroxide (CH), whose formation is linked to strength development in concrete. When silica fume is added to fresh concrete, it chemically reacts with the CH to produce additional CSH. This in turn can enhance compressive strength and chemical resistance. The additional CSH produced by silica fume is more resistant to aggressive chemicals than the weaker CH compounds (Langan et al., 2002). While there have been several attempts to use silica fume in concrete, its application in asphalt pavement has not been studied. While modification with a few nano-materials has been found to be effective, the asphalt industry is very cost sensitive, and the high price of such nano-materials may hinder their application despite their effectiveness.

Selected nano-particles for pavement application should be non-hazardous, low cost, easy to handle, and available in large quantities, regardless of geographical locations. Nano-particles should also fulfil ecological requirements such as low energy consumption and environmental compatibility. Furthermore, they should significantly improve long-term performance and functional properties of the base asphalt (Yildirim, 2007).

Mikoc and Markovic characterized the influence of slag, fly ash, and silica fume on the mechanical and physical properties of asphalt mixtures, using the HRN EN 12697 standard (Markovic and Mikoc, 2010). They concluded that use of slag as an aggregate in asphalt mixtures increases the density and stability of the mixture. The replacement of aggregates and

fillers with waste materials could also lead to cost savings in the production of asphalt mixtures and contribute to its environmental sustainability (You et al., 2011).

Similar research has been performed on high-temperature rheological properties of the binders containing various percentages of carbon nano-particles (Amirkhanian et al., 2010). Their results indicated that the viscosity of binders increased proportionally with the percentage of nano-particles, failure temperature increased in the presence of nano-particles, and the elastic and viscous modulus values increased with the addition of nano-particles.

CHAPTER 3

Preliminary Study

In this chapter, asphalt binder AC 60-70 and silica fume are characterized based on supplier specifications.

3.1 Materials and Methods

The test materials used in this study were asphalt binder penetration grade AC 60-70 and industrial waste silica fume. Four mixtures were made using asphalt 60-70 in the presence of 0.25%, 0.5%, and 1% silica fume. The base binder for this study was penetration grade AC 60-70. Asphalt binder 60-70 is a base binder that is used in high-temperature areas such as Saudi Arabia. The silica fume is considered as an industrial waste material. The Silica fume has physical and chemical properties could lead to improve the mixture properties in terms of stability and density.

3.2 Marshall Test

The Marshall test provides the performance prediction measure for the Marshall mix design method. The stability and flow tests were conducted. The stability portion of the test measures the maximum load supported by the test specimen at a loading rate of 50.8 mm/minute (2 inches/minute). Basically, the load is increased until it reaches a maximum point at which the specimen fails and the load is recorded (Roberts et al., 1996). The test is to determine the stability and flow of compacted samples of asphalt mixture and determine the optimal ratio of asphalt. Samples were immersed in a bath with water temperature of 60 ± 1 ºC and held between 40 and 60 minutes. The samples were then tested using the Marshall stability test. The stability of asphalt samples was determined by the maximum resistance to deformation. The base asphalt used was AC 60-70 in the presence of 0.25%, 0.5%, or 1% silica fume. The stability and flow of

modified specimens were then compared with those measures of control samples without silica fume.

3.3 Mixture Design

Asphalt AC 60-70 was mixed with the stone aggregates following the mix gradation design that is shown in Figure 3-1. Silica fume was then added to the mixture at levels of 0.25%, 0.5, and 1% by weight. Four samples were used in this study. Figure 3-2 shows that six replicates of each sample were considered to ensure significant results. The air weight was measured. Then, the weight of the sample in water was taken. After drying the sample, the S.S.D, which is the saturated surface dry weight, was measured. From the water weight and the S.S.D, the volume was calculated. The density was then calculated using the mass and sample volume. The Marshall test was conducted, and the data of stability and flow were observed. Figure 3-3 shows the Marshall test equipment. Table 3-1 shows the air, water ,and S.S.D weight as well as the Marshal reading of the flow and stability for the mixture sample SFMM100-0. The SFMM refers to Silica Fume Modified Mixture. The 100 is the percentage of asphalt mixture while the 0 is the percentage of silica fume. Tables 3-2, 3-3, and 3-4 show the data of samples that contain 0.25%, 0.5%, and 1% of silica fume, respectively.

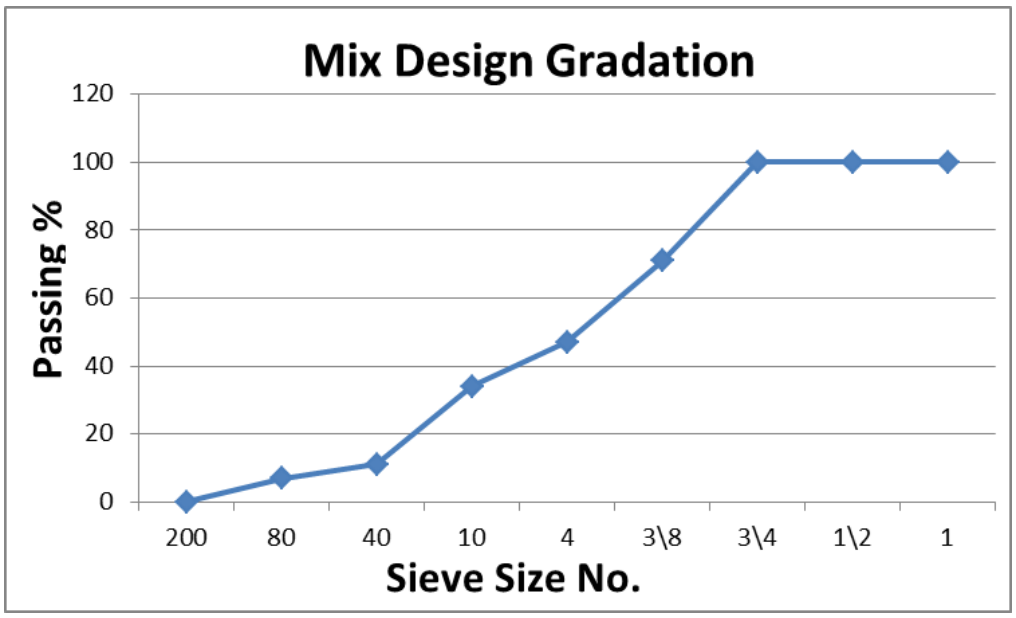

Figure 3-1. Mix Design Gradation

Figure 3-2. Asphalt Mixture Sample Replicates

Figure 3-3. Marshall Test

Table 3-1

Marshall Test for SFMM100-0

Replicate	**1**	**2**	**3**	**4**	**5**	**6**
Air weight	1242.8	1240.1	1231.3	1241.1	1239.7	1237.2
Water weight	742.5	737.8	732.3	742.9	739.9	740.2
S.S.D weight	1252.8	1249.8	1242.5	1252.9	1251.4	1250.6
Volume	510.3	512	510.2	510	511.5	510.4
Density	2.435	2.422	2.413	2.434	2.424	2.424
Ave. flow mm	2.1					
Loss of stability	22.5					

Table 3-2

Marshall Test for SFMM99.75-0.25

Replicate	**1**	**2**	**3**	**4**	**5**	**6**
Air weight	1242.4	1239.7	1236.6.3	1237.4	1231.9	1240
Water weight	743	740.1	739.7	741	734.8	742
S.S.D weight	1254.4	1250.7	1247.8	1248.1	1243.8	1250.3
Volume	510.7	510.6	508.1	507.1	509	508.3
Density	2.433	2.428	2.434	2.440	2.420	2.440
Ave. flow mm	2.5					
Loss of stability	18					

Table 3-3

Marshall Test for SFMM99.5-0.5

Replicate	**1**	**2**	**3**	**4**	**5**	**6**
Air weight	1234.2	1237.5	1240.8	1240.1	1235	1237.7
Water weight	740.2	741.5	742	736	738.1	737.9
S.S.D weight	1249.5	1249.7	1253.4	1247.8	1254.9	1249
Volume	509.3	508.2	511.4	511.8	516.8	511.1
Density	2.423	2.435	2.426	2.423	2.390	2.422
Ave. flow mm	2.6					
Loss of stability	15.1					

Table 3-4

Marshall Test for SFMM99-1

Replicate	**1**	**2**	**3**	**4**	**5**	**6**
Air weight	1238.2	1239.4	1229.2	1239	1236.3	1237.9
Water weight	739.5	740.5	734.6	738.1	738.6	739.4
S.S.D weight	1246.9	1247.0	1238.4	1246.6	1244.6	1245.9
Volume	507.4	506.5	503.8	508.5	506	506.5
Density	2.440	2.447	2.440	2.437	2.443	2.444
Ave. flow mm	2.63					
Loss of stability	12.2					

3.4 Stability and Flow

Introduction of silica fume decreased the loss of stability; as the percentages of silica fume increased, the loss of stability decreased, as shown in Figure 3-4. The loss of stability was reduced by 20% when 0.25% silica fume was added to the mixture. In the presence of 0.5% silica fume, the loss of stability was reduced by 33%, while the addition of 1% silica fume to the asphalt mixture reduced the loss of stability by 46%. A more stable mixture can lead to more resistance to rutting. Figure 3-5 shows that the flow increased by 19% when 0.25% of silica fume was introduced to the mixture. Furthermore, the flow number continued to increase to reach 25% as the silica fume percentage increased to 1%. Consequently, by adding silica fume to the asphalt mixture, the mixture becomes more workable.

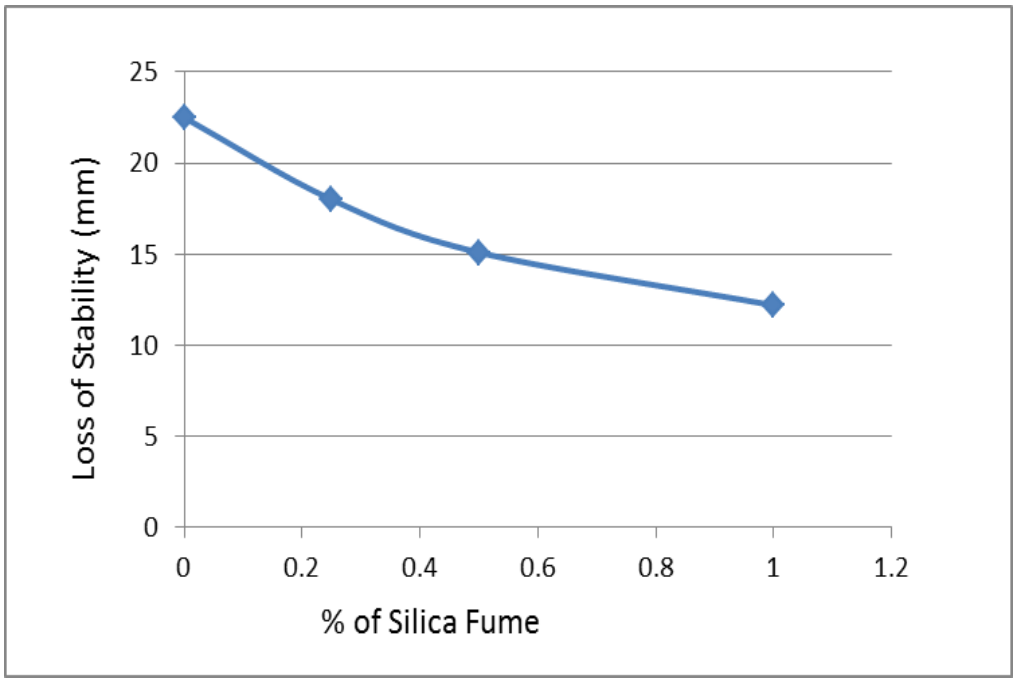

Figure 3-4. Loss of Stability vs. Percentage of Silica Fume

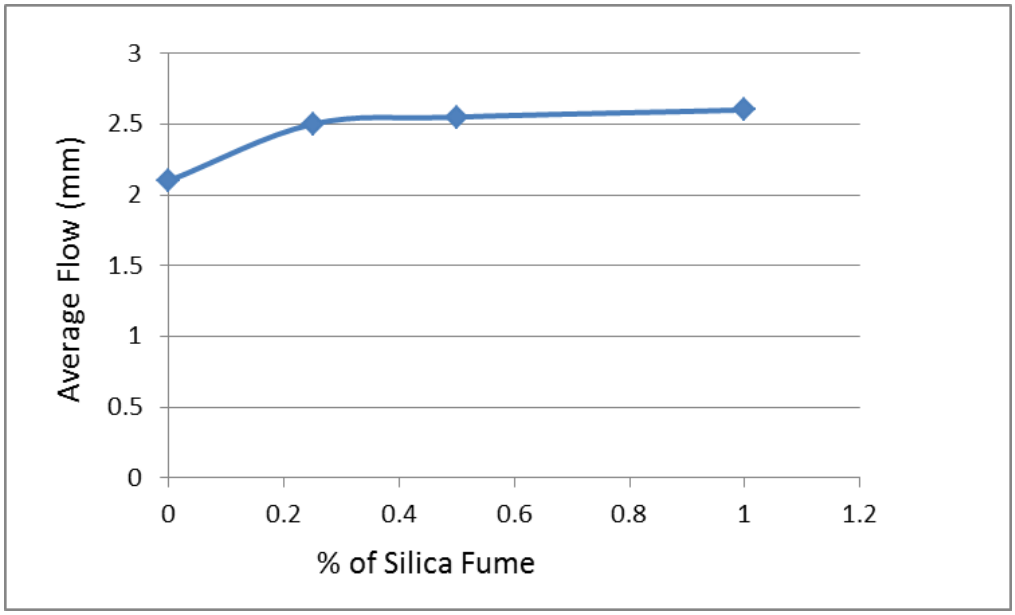

Figure 3-5. Average Flow vs. Percentage of Silica Fume

CHAPTER 4

Methodology

In this chapter, asphalt binder PG 64-22 and silica fume are characterized.

4.1 Materials and Methods

The test materials used in this study were asphalt binder penetration grade PG 64-22 and industrial waste silica fume. The silica fume concentrations in asphalt binder PG 64-22 were selected to be 2%, 4%, and 8%, for both aged and non-aged samples.

4.1.1 Asphalt binders

The base binders for this study were penetration grade PG 64-22. Asphalt binder PG 64-22 is commonly used in North Carolina.

4.1.2 Silica fume

The silica fume used in this study was acquired through Norchem Company, located in Hauppauge, NY. Table 4-1 shows the chemical composition of the silica fume used in this study. Silica fume consists of amorphous silica that is produced by electric arc furnaces as a byproduct of the production of elemental silicon or ferro silicon alloys (Gapinski and Scanlon, 2011). The silica fume has 100nm – 200nm average particle size, as shown in Figure 4-1. Figure 4-2 shows a scanning electron microscopy (SEM) image that indicates fine particles of silica fume of less than 300 nm in diameter (Haipeng, 2014). Silica fume is an extremely fine material that is considered as a nano-material. The particle size of silica fume is approximately 100 times smaller than the average size of cement particles. Silica fume surface area ranges from 60,000 to 150,000 ft^2/lb or 13,000 to 30,000 m^2/kg. Its specific gravity is 2.2. The main constituent material in silica fume is silica ($Si0_2$) (FHWA, 2012).

Table 4-1

Chemical Composition of Silica Fume

Chemical	Composition %	Chemical	Composition %
Silicon Dioxide (SiO_2)	90.26	Sodium Oxide (Na_2O)	0.60
Aluminum Oxide (Al_2O_3)	0.13	Potassium Oxide (K_2O)	1.34
Iron Oxide (Fe_2O_3)	2.46	Sulfur trioxide (SO_3)	0.29
Calcium Oxide (CaO)	0.29	Others	0.26
Magnesium Oxide (MgO)	1.57	Loss on ignition	2.80

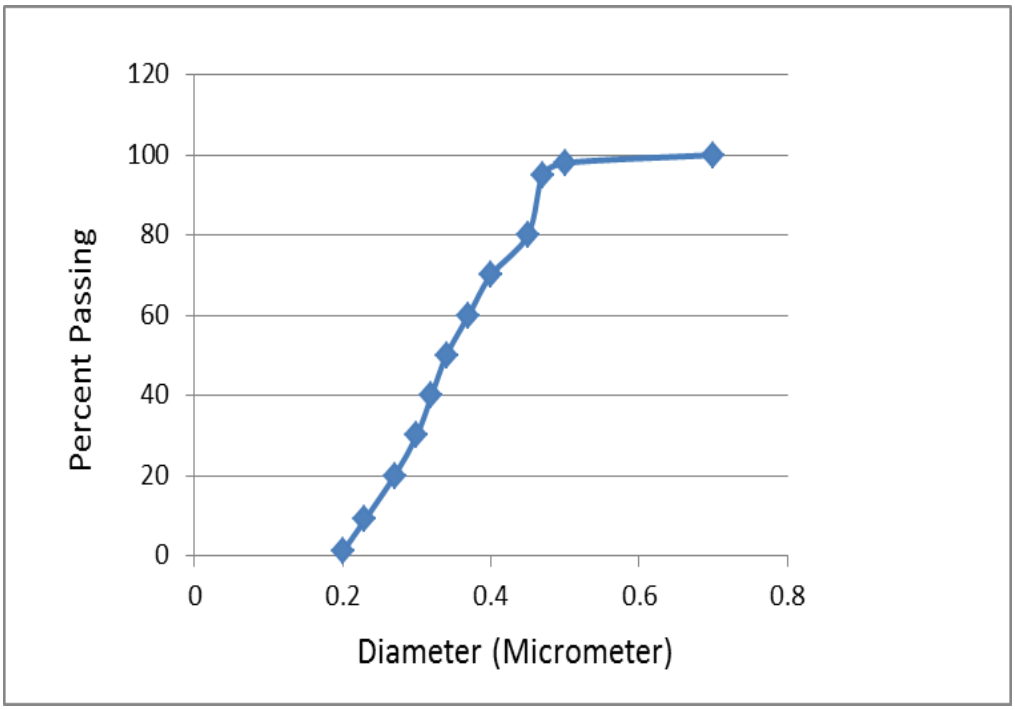

Figure 4-1. Silica Fume Particle Size Distribution

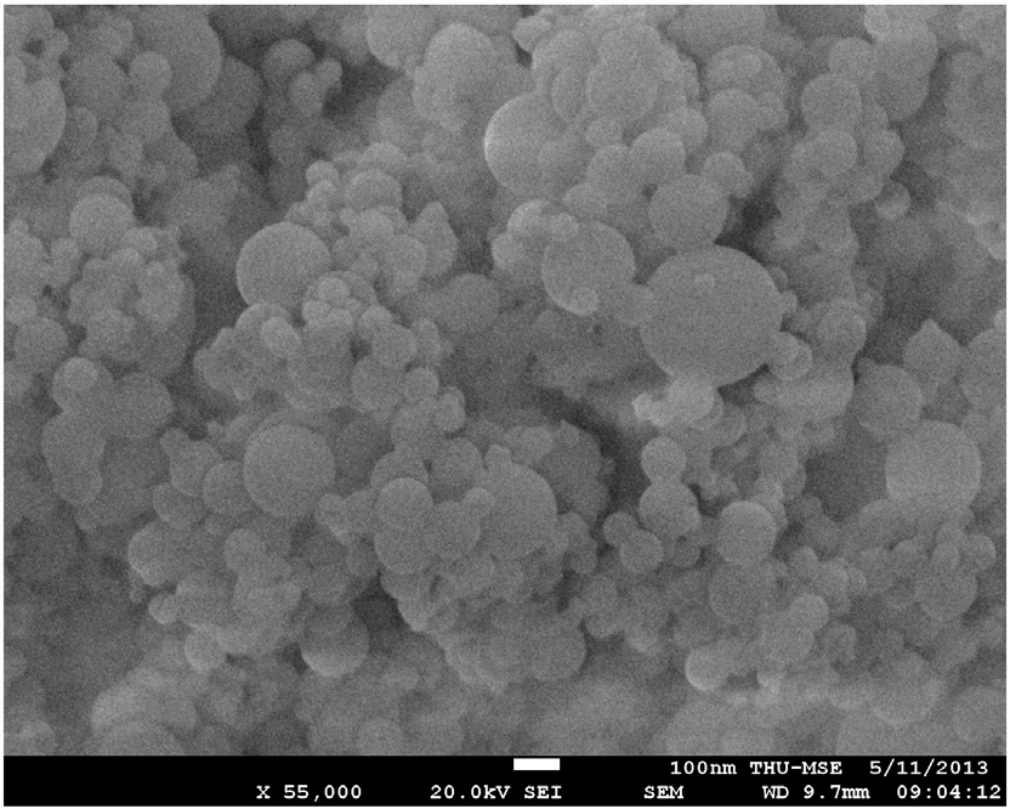

Figure 4-2. Silica Fume Particle Shape (Haipeng, 2014)

4.2 Viscosity Measurement

The rotational viscometer (RV) tests were conducted utilizing a Brookfield DV-III Ultra viscometer equipped with thermosel to control temperature. The basic RV test measures torque required to maintain a constant rotational speed of a specified spindle (in this study, spindle SC27 was used) submerged in liquid asphalt at a constant temperature. The data is then used to calculate viscosity from a measured torque. The viscosity of non-aged samples in the presence of various amounts of silica fume (2%, 4%, and 8%) was measured by viscometer, following the ASTM D4402 specification. Viscosity was measured at four different temperatures (105˚C, 120˚C, 135˚C, 150˚C), and six different speeds (5, 10, 20, 25, 50, and 75 RPM). At each temperature, the reading was recorded after every 30 minutes.

4.3 Fourier Transform Infrared Spectroscopy (FTIR)

FTIR analysis was used to characterize silica-fume-modified asphalts. An FTIR spectrometer, Shimadzu 1.30(2005) single reflection zinc selenide prism, was used in transmission mode. In wave-numbers ranging from 4000/cm to 500/cm, the test was conducted to get the spectra of asphalt samples. The prism was cleaned with methylene chloride. The frequencies of IR radiation ("peaks" or "signals") could be linked directly to the bond type. Each bond vibrates in different motions (stretching or bending); individual bonds may absorb different IR frequencies. Stretching absorptions usually produce stronger peaks than bending, however, the weak absorptions can be useful in differentiating similar types of bonds (e.g. aromatic substitution). Table 4-2 is an example of some of the bonds and related absorption.

Table 4-2

Description of IR Absorptions (TutorVista, 2013)

Bond	Compound Type	Frequency Range, cm-1
C-H	Alkanes	2960-2850 (s) stretch
	CH; Umbrella Deformation	1470-1350 (v) scissoring and bending
		1380 (m-w) - Doublet - isopropyl, t-butyl
C-H	Alkanes	3080-3020 (m) stretch
		1000-675 (s) bend
C-H	Aromatic Rings	3100-3000 (m) stretch
	Phenyl Ring Substitution Bands	870-675 (s) bend
	Phenyl Ring Substitution Overtones	2000-1600 (w) - fingerprint region
C-H	Alkanes	3333-3267 (s) stretch
		700-610 (b) bend
C=C	Alkenes	1680-1640 (m,w) stretch
C°C	Alkynes	2260-2100 (w,sh) stretch
C=C	Aromatic Rings	1600, 1500 (w) stretch
C-O	Alcohols, Ethers, Caroxylic acids, Esters	1260-1000 (s) stretch
C=O	Aldehydes, Ketones, Carboxylic acids, Esters	1760-1670 (s) stretch
O-H	Monomeric -- Alcohols, Phenol	3640-3160 (s,br) stretch
	Hydrogen-bonded -- Alcohols, Phenols	3600-3200 (b) stretch
	Carboxylic acids	3000-2500 (b) stretch
N-H	Amines	3500-3300 (m) stretch
		1650-1580 (m) bend
C-N	Amines	1340-1020 (m) bend
C°N	Nitriles	2260-2220 (v) stretch
NO2	Nitro Compounds	1660-1500 (s) asymmetrical stretch
		1390-1260 (s) symmetrical stretch

4.4 Aging Procedure

Short-term laboratory aging of the binders was performed using a Rolling Thin Film Oven (RTFO) procedure. The RTFO procedure was executed in accordance with ASTM D2872-13.

4.5 X-Ray Diffraction Test

XRD is a significant technique to examine the exfoliation of nano-particles in asphalt binders. This test is used to demonstrate a material's polycrystalline structure. It identifies components in a sample by search/match procedure. This tool is used to identify the atoms and molecular structure in the crystal. From the density of the electron produced by the crystallographer, the position of the atoms can be calculated, as well as the chemical bonds. (Barbara and Clark, 2013). All samples were placed in an oven at 150ºC until a homogeneous liquid phase was attained. A small portion was then placed in a silver sample holder (eight mm each in diameter). Each specimen was carefully examined to identify any bulge or irregularity on the surface. The sample-A glass plate was used to trim any excess sample off the top of the specimen. The sample holder was then placed on a flat surface, and the samples were loaded onto the tray. The specimens were left to cure at room temperature before running the test. After curing, the samples were placed on an eight-shelf holster and set in the correct position for testing to take place.

4.6 Mixture Design

PG 64-22 was placed in a typical oven at 200˚C until it reaches a homogeneous liquid phase. There are twelve mixtures designed in this research, 250 grams of each mixture. Table 4-3 indicates the experiment mixture design of the binder level study. 8 Samples were conducted using silica fume modified binder. ASFMA is an abbreviation for Aged Silica-Fume-Modified

Asphalt; NSFMA is an abbreviation for Non-aged Silica-Fume-Modified Asphalt. The numbers appended to ASFMA or NSFMA indicate the percentage of asphalt binder followed by the percentage of silica fume.

Table 4-3

Experiment Mixture Design

	Aged (RTFO)		**Non-Aged**	
	Control (PG 64-22)	**Silica Fume**	**Control (PG 64-22)**	**Silica Fume**
ASFMA100-0	100%	0%		
ASFMA98-2	98%	2%		
ASFMA96-4	96%	4%		
ASFMA92-8	92%	8%		
NSFMA100-0			100%	0%
NSFMA98-2			98%	2%
NSFMA96-4			96%	4%
NSFMA92-8			92%	8%

4.6.1 Silica fume

The mixture including 2% silica fume contains 245 grams of PG 64-22. These 245 grams of PG 64-22 were placed on a heating plate. The heating plate was set to 200˚C, where the blending took place. A drill with a mixing attachment was used to blend. Blending time was 30 minutes, where 5 grams of silica fume (2%) was poured into the PG 64-22 (245 grams) asphalt binder momentarily. This procedure was then repeated for the remaining two mixture designs. For 4% silica fume, 10 grams of silica fume was gradually added to 240 grams of PG 64-22 asphalt binder over a heating plate at 200˚C. For 8% silica fume, 20 grams of silica fume was gradually added to 230 grams of PG 64-22 asphalt binder over a heating plate at 200˚C.

4.7 Sample Preparation

4.7.1 Rotational viscosity test

To gain a significant sampling of the blend, 10 plus or minus 5 grams of each material was poured into different aluminum chambers. The tubes were then placed into a 30 minute pre-heated thermosel to reach thermal equilibrium. Figure 4-3 shows the conventional oven that was used to preheat all specimens.

Figure 4-3. Conventional Oven to Heat the Sample

To investigate properties of the silica fume samples, the tests were run at 105 ˚C, 120 ˚C, 135 ˚C, and 150 ˚C at speeds of 5,10, 20, 25, 50, 75 and 100 rpm. The samples were preheated at their designated temperature for an additional 20 minutes to ensure achievement of thermal equilibrium. Spindle SC27 was used for testing. The first viscosity reading was conducted after 15 minutes of shearing, then three more recordings were done at 3 minute intervals to ensure consistency of viscosity measurements. Figure 4-4 is a graphical representation of the blending mechanism used to mix silica fume with base asphalt PG 64-22. Figure 4-5 is the Brookfield rotational viscometer.

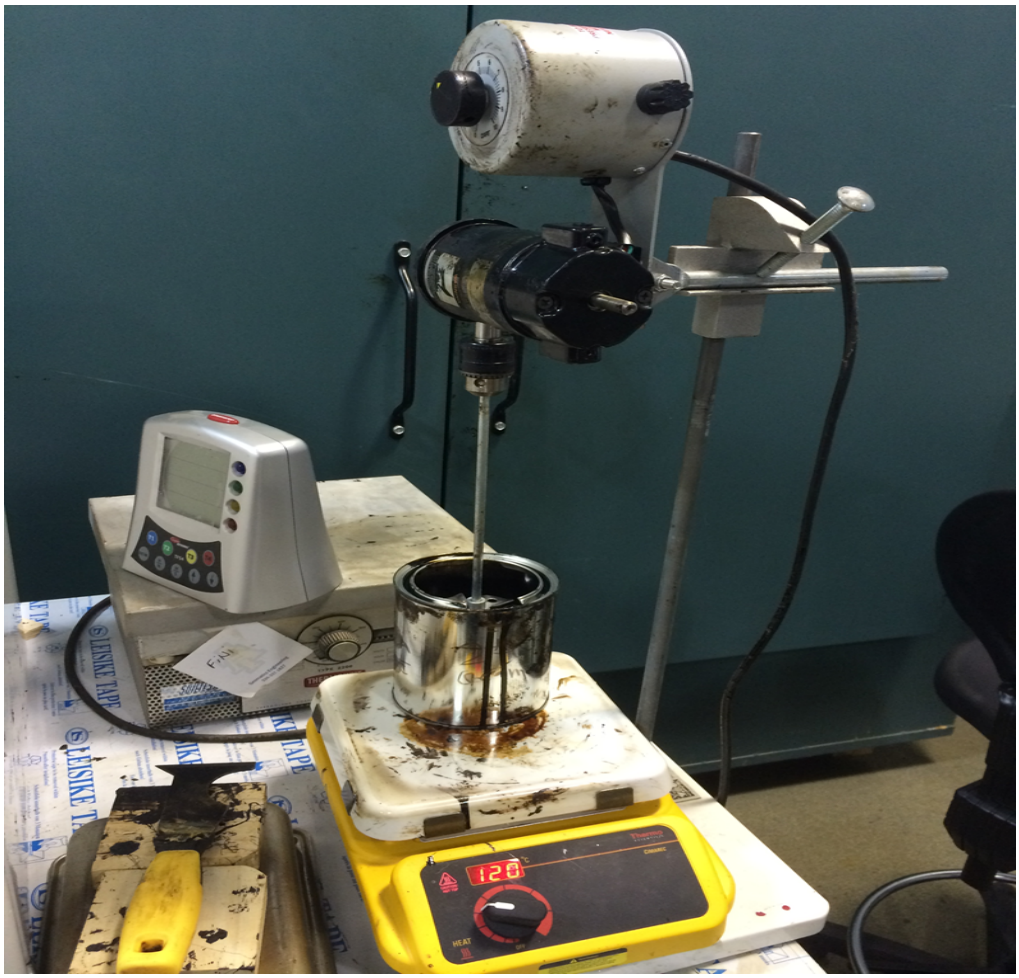

Figure 4-4. The Bench-top High Shear Mixer Used for Blending

Figure 4-5. Brookfield Rotational Viscometer (RV)

4.7.2 X-ray diffraction test

All samples were placed in an oven at 150ºC until reaching a homogeneous liquid phase. Then, a small portion was placed in a sample holder with a diameter of eight mm. Each specimen was examined to identify any irregularities on the surface. The sample glass plate was used to trim any excess sample off the top of the specimen. Then, the sample holder was placed on a flat surface and the samples were loaded onto the tray. The specimens were left to cure at room temperature before running the test. When all samples were prepared appropriately, they were placed on an eight shelf holster that was associated with the diffractometer, and then set in the correct position for the test to take place. The diffractometer is shown in Figure 4-6. The anchor scan parameters for the x-ray diffraction test are shown in Table 4-4.

Figure 4-6. Diffractometer System XPERT-PRO

Table 4-4

Anchor Scan Parameters for X-ray Diffraction Test

Anchor Scan Parameters	
Start Position [° 2θ]	4.0084
End Position [° 2θ]	59.9894
Step Size [° 2θ]	0.0170
Scan Step Time [s]	269.8750
Scan Type	Continuous
Divergence Slit Type	Automatic
Irradiated Length [mm]	6.0000
Specimen Length [mm]	10.0000
Measurement Temperature [°C]	25.0000
Anode Material	Cu
K-Alpha1 [Å]	1.5406
K-Alpha2 [Å]	1.5444
K-Beta [Å]	1.3922
Generator Settings	40mA, 45kV
Spinning	Yes

4.7.3 Fourier transform infrared test

These samples were prepared at room temperature. A toothpick was used to remove a small portion of a sample in its solid state and smear it onto the sample holder, which was transparent with a convex surface. The sample was analyzed by a fully-computerized Fourier Transform Infrared Spectroscopy system that generates a spectrum showing the molecular structure of the sample material. Absorbance peaks on the spectrum indicate functional groups. The analytical spectrum is then compared in a reference library program with cataloged spectra to identify components or to find a “best match” for unknown material using the cataloged spectra for known materials.

CHAPTER 5

Results

All analysis and results from this study are discussed in this chapter. Graphs and procedures are used to help illustrate each specimen as it is compared with other specimens. Tests were run at the North Carolina A&T State University Civil Engineering Lab and the Laboratory for Atomistic and Molecular Mechanics (LAMM) as well as the Center for Materials Science and Engineering at MIT (CMSE) lab.

5.1 Viscosity Measurement Before Aging

At a shear rate of 10 rpm, Figure 5-1 shows that at each temperature, the viscosity measurement results indicate a significant increase of viscosity due to the addition of silica fume. At 105°C, the viscosity increased by 25% when 2% silica fume was added to the control asphalt binder PG 64-22. The viscosity increased by 38% and 58% when silica fume was increased 4% and 8%, respectively. At 120°C, the presence of 8% silica fume in modified asphalt binder resulted in a 40% increase in the viscosity. At 135°C, which is the standard temperature, a 2% decrease in viscosity was found when 2% of silica fume was introduced to the control asphalt binder. When 4% silica fume was added to the control binder, the viscosity increased by 25%, while adding 8% silica fume increased the viscosity by 40%. At a high temperature of 150°C, the viscosity increased by 15%, 40%, and 59% when 2%, 4% and 8% silica fume was added, respectively. The data is shown in Table 5-1.

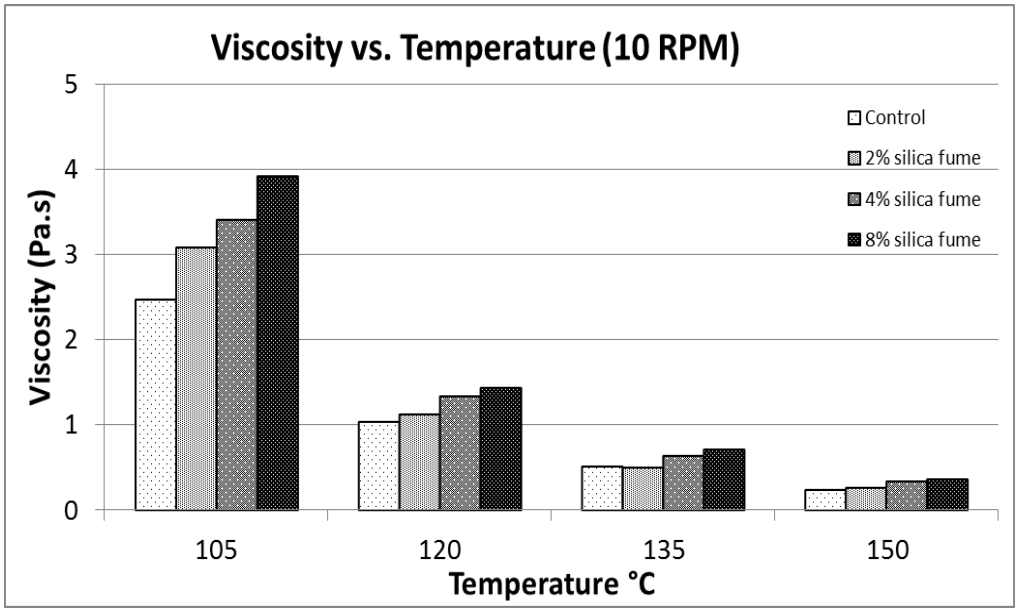

Figure 5-1. Viscosity vs. Temperature (°C) at 10 rpm (Before Aging)

Table 5-1

Viscosity Measurements of Non-Aged Samples at 10 rpm

Temp (°C)	Viscosity	Non-Modified PG 64-22	Silica fume Modified			Viscosity Variation		
			2%	4%	8%	2%	4%	8%
105	v1	2450.0	3100.0	3425.0	3925.0	26.5	39.8	60.2
	v2	2475.0	3075.0	3400.0	3900.0	24.2	37.4	57.6
	v3	2475.0	3050.0	3375.0	3900.0	23.2	36.4	57.6
	Average	2466.7	3075.0	3400.0	3908.3	24.7	37.8	58.4
	Stedv	14.4	25.0	25.0	14.4			
	Cov	0.0	0.0	0.0	0.0			
120	v1	1025.0	1100.0	1325.0	1450.0	7.3	29.3	41.5
	v2	1025.0	1125.0	1350.0	1425.0	9.8	31.7	39.0
	v3	1025.0	1125.0	1300.0	1400.0	9.8	26.8	36.6
	Average	1025.0	1116.7	1325.0	1425.0	8.9	29.3	39.0
	Stedv	0.0	14.4	25.0	25.0			
	Cov	0.0	0.0	0.0	0.0			
135	v1	500.0	475.0	600.0	700.0	-5.0	20.0	40.0
	v2	500.0	500.0	625.0	675.0	0.0	25.0	35.0
	v3	500.0	500.0	650.0	725.0	0.0	30.0	45.0
	Average	500.0	491.7	625.0	700.0	-1.7	25.0	40.0
	Stedv	0.0	14.4	25.0	25.0			
	Cov	0.0	0.0	0.0	0.0			
150	v1	225.0	250.0	325.0	375.0	11.1	44.4	66.7
	v2	225.0	275.0	300.0	350.0	22.2	33.3	55.6
	v3	225.0	250.0	350.0	350.0	11.1	55.6	55.6
	Average	225.0	258.3	325.0	358.3	14.8	44.4	59.3
	Stedv	0.0	14.4	25.0	14.4			
	Cov	0.0	0.1	0.1	0.0			

At a shear rate of 20 rpm, Figure 5-2 shows that at each temperature, the viscosity measurement results indicate a significant increase of viscosity due to the addition of silica fume. It can be seen at 105°C that with the addition of 2% silica fume to the control binder, the viscosity increased by 23%, while adding 8% silica fume increased the viscosity by 56%. At 120°C, the viscosity increased by 15% when 2% silica fume was introduced to the control asphalt binder, while adding 4% and 8% silica fume increased the viscosity by 34% and 43%, respectively. At 135°C, which is the standard temperature, a 4% increase in viscosity was found when 2% silica fume was introduced to the control asphalt binder. When 4% silica fume was added to the control binder, the viscosity increased by 24%, while adding 8% silica fume increased the viscosity by 40%. At a high temperature of 150°C, the viscosity increased by 18%, 41%, and 55% when 2%, 4% and 8% silica fume was added, respectively. The data is shown in Table 5-2.

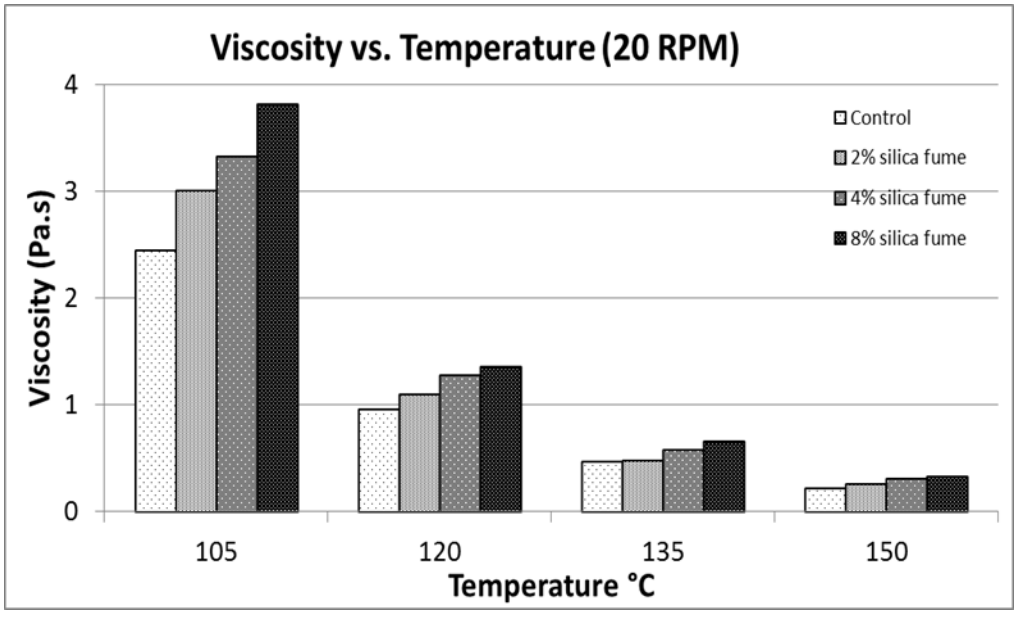

Figure 5-2. Viscosity vs. Temperature (°C) at 20 rpm (Before Aging)

Table 5-2

Viscosity Measurements of Non-Aged Samples at 20 rpm

Temp (°C)	Viscosity	Non-Modified PG 64-22	Silica fume Modified			Viscosity Variation		
			2%	4%	8%	2%	4%	8%
105	v1	2438.0	3000.0	3350.0	3800.0	23.1	37.4	55.9
	v2	2438.0	3000.0	3313.0	3805.0	23.1	35.9	56.1
	v3	2450.0	3013.0	3300.0	3813.0	23.0	34.7	55.6
	Average	2442.0	3004.3	3321.0	3806.0	23.0	36.0	55.9
	Stedv	6.9	7.5	25.9	6.6			
	Cov	0.0	0.0	0.0	0.0			
120	v1	950.0	1100.0	1263.0	1388.0	15.8	32.9	46.1
	v2	950.0	1088.0	1280.0	1305.0	14.5	34.7	37.4
	v3	950.0	1088.0	1278.0	1375.0	14.5	34.5	44.7
	Average	950.0	1092.0	1273.7	1356.0	14.9	34.1	42.7
	Stedv	0.0	6.9	9.3	44.6			
	Cov	0.0	0.0	0.0	0.0			
135	v1	462.5	475.0	575.0	637.0	2.7	24.3	37.7
	v2	462.5	487.5	587.0	650.0	5.4	26.9	40.5
	v3	462.5	475.0	562.0	662.5	2.7	21.5	43.2
	Average	462.5	479.2	574.7	649.8	3.6	24.3	40.5
	Stedv	0.0	7.2	12.5	12.8			
	Cov	0.0	0.0	0.0	0.0			
150	v1	212.5	250.0	300.0	325.0	17.6	41.2	52.9
	v2	212.5	250.0	287.0	325.0	17.6	35.1	52.9
	v3	212.5	250.0	312.0	337.5	17.6	46.8	58.8
	Average	212.5	250.0	299.7	329.2	17.6	41.0	54.9
	Stedv	0.0	0.0	12.5	7.2			
	Cov	0.0	0.0	0.0	0.0			

When a higher shear rate of 50 rpm was used, Figure 5-3 shows the results were consistent. At 105°C, the viscosity increased by 22% when 2% silica fume was introduced to the control asphalt binder. In the presence of 4% silica fume, the viscosity increased by 35%, while

the viscosity increased by 52% when 8% silica fume was added. At a temperature of 120°C, the viscosity increased by 17%, 32%, and 46% when 2%, 4%, and 8% of silica fume was added, respectively. As the percentage of silica fume increased, so did the viscosity. At 135°C, it was shown that viscosity increased by 12% in the presence of 2% silica fume. The viscosity increased by 30% when 4% silica fume was added. 8% of silica fume resulted in a 48% increase in viscosity. At 150°C, viscosity increased by 13%, 29%, and 44% when silica fume was added at 2%, 4%, and 8%, respectively. The data is shown in Table 5-3.

However, overall binder viscosity measurements at 50 rpm were lower than those measured at 10 rpm, confirming that measurements were sensitive to the change in shear rate.

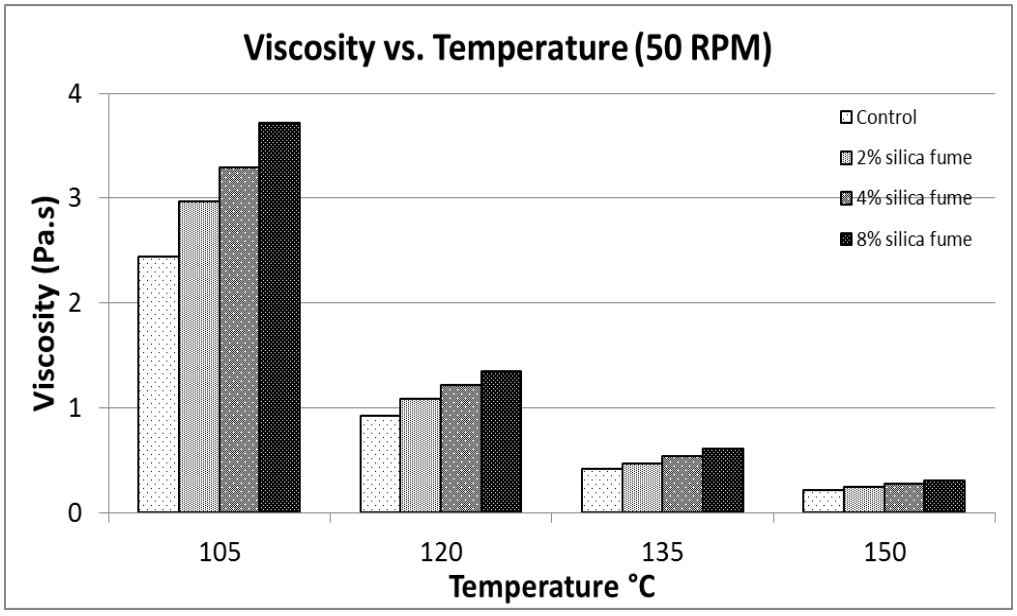

Figure 5-3. Viscosity vs. Temperature (°C) at 50 rpm (Before Aging)

Table 5-3

Viscosity Measurements of Non-Aged Samples at 50 rpm

Temp (°C)	Viscosity	Non-Modified PG 64-22	Silica fume Modified			Viscosity Variation		
			2%	4%	8%	2%	4%	8%
105	v1	2435.0	2965.0	3290.0	3720.0	21.8	35.1	52.8
	v2	2430.0	2960.0	3285.0	3700.0	21.8	35.2	52.3
	v3	2440.0	2960.0	3290.0	3715.0	21.3	34.8	52.3
	Average	2435.0	2961.7	3288.3	3711.7	21.6	35.0	52.4
	Stedv	5.0	2.9	2.9	10.4			
	Cov	0.0	0.0	0.0	0.0			
120	v1	920.0	1075.0	1215.0	1345.0	16.8	32.1	46.2
	v2	920.0	1080.0	1220.0	1340.0	17.4	32.6	45.7
	v3	920.0	1080.0	1210.0	1350.0	17.4	31.5	46.7
	Average	920.0	1078.3	1215.0	1345.0	17.2	32.1	46.2
	Stedv	0.0	2.9	5.0	5.0			
	Cov	0.0	0.0	0.0	0.0			
135	v1	415.0	465.0	535.0	605.0	12.0	28.9	45.8
	v2	415.0	470.0	540.0	612.0	13.3	30.1	47.5
	v3	415.0	465.0	540.0	610.0	12.0	30.1	47.0
	Average	415.0	466.7	538.3	609.0	12.4	29.7	46.7
	Stedv	0.0	2.9	2.9	3.6			
	Cov	0.0	0.0	0.0	0.0			
150	v1	210.0	235.0	270.0	300.0	11.9	28.6	42.9
	v2	210.0	240.0	270.0	300.0	14.3	28.6	42.9
	v3	210.0	240.0	275.0	305.0	14.3	31.0	45.2
	Average	210.0	238.3	271.7	301.7	13.5	29.4	43.7
	Stedv	0.0	2.9	2.9	2.9			
	Cov	0.0	0.0	0.0	0.0			

5.2 Rolling Thin-Film Oven (RTFO)

The Rolling Thin-Film Oven (RTFO), shown in Figure 5-4, represents short-term oxidation aging. It is used to simulate the aging process in the field in terms of air and

temperature. The RTFO procedure was executed in accordance with ASTM D2872-13. To start the method of short-term aging using the RTFO, the following procedure was used. The samples of control asphalt binder, 2%, 4%, and 8% silica-fume-modified binder were pre-heated for 4 hours. Then, 35.5g of each asphalt sample was poured into each glass bottle. After that, the bottles were rotated and placed at room temperature to cool for 60 to 180 minutes. The bottles were placed in a circular metal carriage in the RTFO oven carousel, shown in Figure 5-5. While maintaining the oven temperature at 163°C and the airflow into the bottles at 4000 ml/min., the carousel was rotated at 15 RPM for 85 minutes. As a result, the samples became aged in terms of air and temperature.

Figure 5-4. Rolling Thin-Film Oven (RTFO)

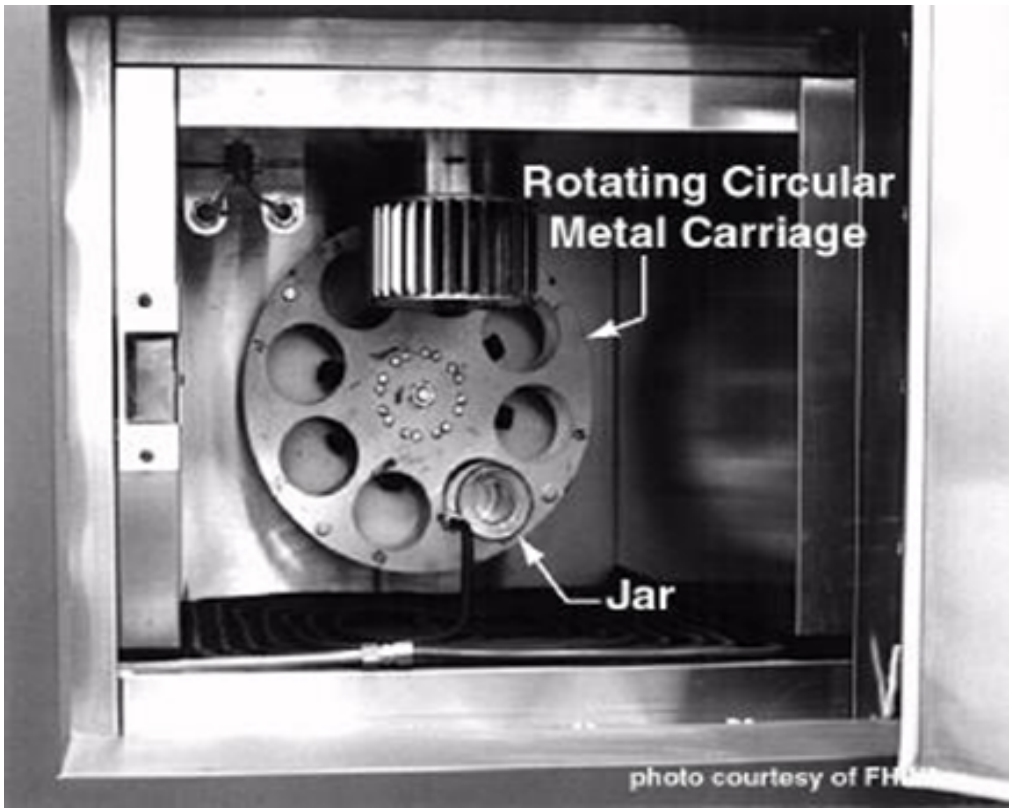

Figure 5-5. Rotating Circular Metal Carriage

5.3 Viscosity Measurement after Aging

Figure 5-6 shows the rotational viscosity results of modified and non-modified specimens after RTFO aging, when tested at 10 rpm. It can be seen at 105°C that with the addition of 2% silica fume to the control binder, the viscosity decreased by 7%, while adding 8% silica fume increased the viscosity by 21%. At 120°C, the viscosity decreased by 2% when 2% silica fume was introduced to the control asphalt binder, while adding 4% and 8% silica fume increased the viscosity by 7% and 21%, respectively. At 135°C, which is the standard temperature, a 7% decrease in viscosity was found when 2% silica fume was introduced to the control asphalt binder. When 4% silica fume was added to the control binder, the viscosity increased by 10%, while adding 8% silica fume increased the viscosity by 27%. At a high temperature of 150°C, the

viscosity increased by 15%, 13%, and 28% when 2%, 4%, and 8% silica fume was added, respectively. The data is shown in Table 5-4.

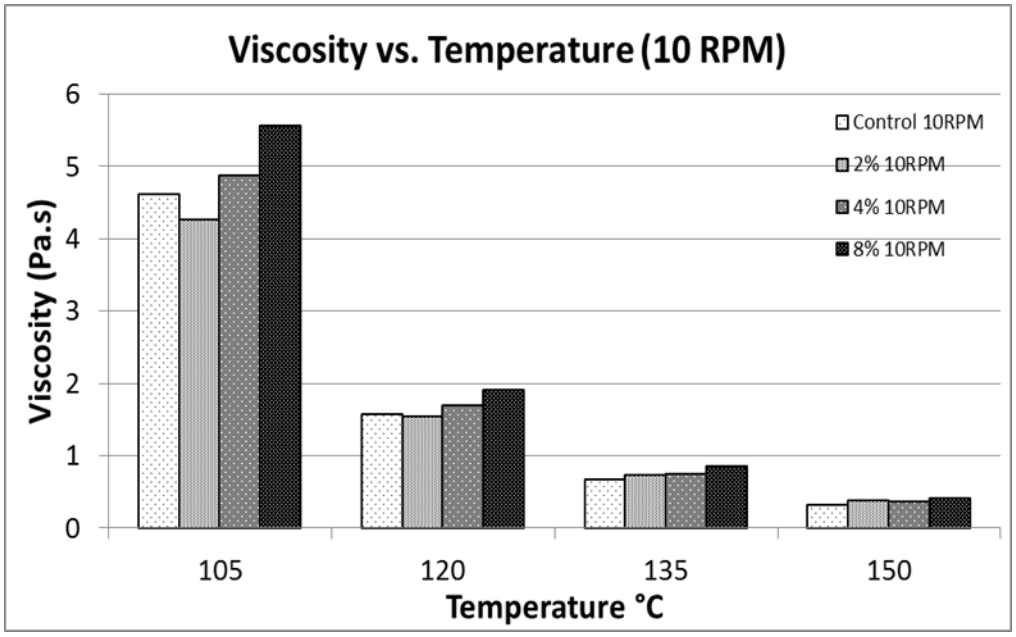

Figure 5-6. Viscosity vs. Temperature (°C) at 10 rpm (After Aging)

Table 5-4

Viscosity Measurements of Aged Samples at 10 rpm

Temp (°C)	Viscosity	Non-Modified PG 64-22	Silica fume Modified			Viscosity Variation		
			2%	4%	8%	2%	4%	8%
105	v1	4650.0	4300.0	4875.0	5550.0	-7.5	4.8	19.4
	v2	4600.0	4275.0	4900.0	5600.0	-7.1	6.5	21.7
	v3	4600.0	4250.0	4875.0	5550.0	-7.6	6.0	20.7
	Average	4616.7	4275.0	4883.3	5566.7	-7.4	5.8	20.6
	Stedv	28.9	25.0	14.4	28.9			
	Cov	0.0	0.0	0.0	0.0			
120	v1	1575.0	1550.0	1700.0	1950.0	-1.6	7.9	23.8
	v2	1600.0	1550.0	1700.0	1900.0	-3.1	6.3	18.8
	v3	1575.0	1550.0	1700.0	1900.0	-1.6	7.9	20.6
	Average	1583.3	1550.0	1700.0	1916.7	-2.1	7.4	21.1
	Stedv	14.4	0.0	0.0	28.9			
	Cov	0.0	0.0	0.0	0.0			
135	v1	700.0	725.0	750.0	850.0	3.6	7.1	21.4
	v2	675.0	750.0	750.0	875.0	11.1	11.1	29.6
	v3	675.0	725.0	750.0	875.0	7.4	11.1	29.6
	Average	683.3	733.3	750.0	866.7	7.3	9.8	26.8
	Stedv	14.4	14.4	0.0	14.4			
	Cov	0.0	0.0	0.0	0.0			
150	v1	325.0	375.0	375.0	425.0	15.4	15.4	30.8
	v2	350.0	400.0	375.0	425.0	14.3	7.1	21.4
	v3	325.0	375.0	375.0	425.0	15.4	15.4	30.8
	Average	333.3	383.3	375.0	425.0	15.0	12.5	27.5
	Stedv	14.4	14.4	0.0	0.0			
	Cov	0.0	0.0	0.0	0.0			

Figure 5-7 shows the rotational viscosity results of modified and non-modified specimens after RTFO aging, when tested at 20 rpm. At 105°C, viscosity decreased by 7% when 2% silica fume was introduced to the control asphalt binder, PG 64-22. Viscosity increased by 6% and 20% when silica fume was added at 4% and 8%, respectively. At 120°C, the presence of 8%

silica-fume-modified asphalt binder resulted in a 20% increase in the viscosity. At 135°C ,which is the standard temperature, a 0.6% decrease in viscosity was found when 2% silica fume was introduced to the control asphalt binder. When 4% silica fume was added to the control binder, viscosity increased by 8%, while adding 8% silica fume increased viscosity by 22%. At a high temperature of 150°C, viscosity increased by 5%, 10%, and 23% when 2%, 4% and 8% silica fume was added, respectively. The data is shown in Table 5-5.

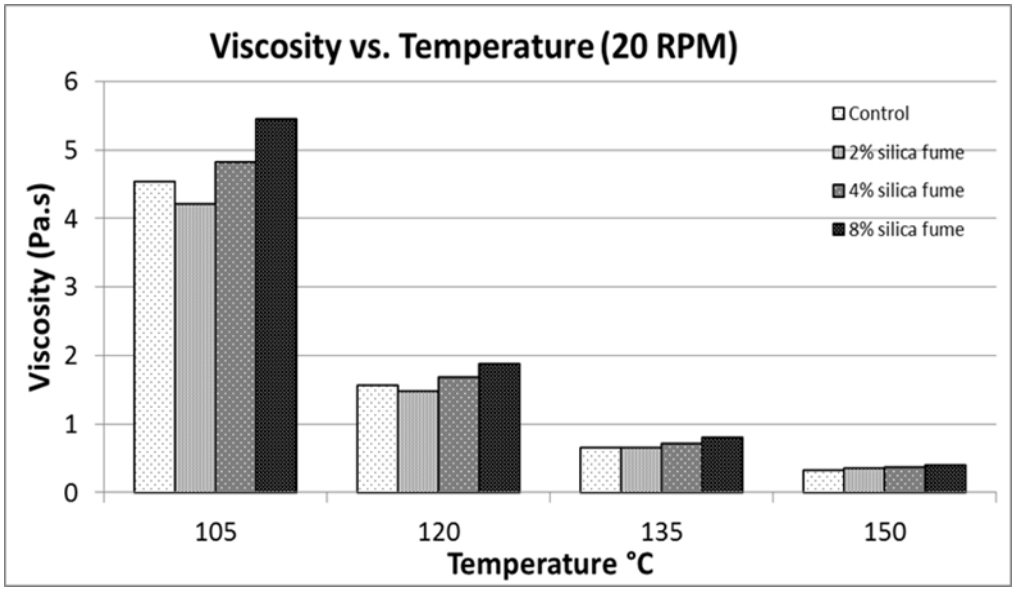

Figure 5-7. Viscosity vs. Temperature (°C) at 20 rpm (After Aging)

Table 5-5

Viscosity Measurements of Aged Samples at 20 rpm

Temp (°C)	Viscosity	Non-Modified PG 64-22	Silica fume Modified			Viscosity Variation		
			2%	4%	8%	2%	4%	8%
105	v1	4550.0	4213.0	4838.0	5475.0	-7.4	6.3	20.3
	v2	4550.0	4200.0	4825.0	5463.0	-7.7	6.0	20.1
	v3	4550.0	4225.0	4825.0	5463.0	-7.1	6.0	20.1
	Average	4550.0	4212.7	4829.3	5467.0	-7.4	6.1	20.2
	Stedv	0.0	12.5	7.5	6.9			
	Cov	0.0	0.0	0.0	0.0			
120	v1	1563.0	1475.0	1688.0	1880.0	-5.6	8.0	20.3
	v2	1563.0	1488.0	1675.0	1875.0	-4.8	7.2	20.0
	v3	1575.0	1463.0	1675.0	1875.0	-7.1	6.3	19.0
	Average	1567.0	1475.3	1679.3	1876.7	-5.8	7.2	19.8
	Stedv	6.9	12.5	7.5	2.9			
	Cov	0.0	0.0	0.0	0.0			
135	v1	662.5	662.5	712.5	812.0	0.0	7.5	22.6
	v2	650.0	650.0	712.5	800.0	0.0	9.6	23.1
	v3	662.5	650.0	712.5	800.0	-1.9	7.5	20.8
	Average	658.3	654.2	712.5	804.0	-0.6	8.2	22.1
	Stedv	7.2	7.2	0.0	6.9			
	Cov	0.0	0.0	0.0	0.0			
150	v1	325.0	350.0	362.0	400.0	7.7	11.4	23.1
	v2	325.0	337.0	362.0	412.0	3.7	11.4	26.8
	v3	337.5	350.0	362.0	400.0	3.7	7.3	18.5
	Average	329.2	345.7	362.0	404.0	5.0	10.0	22.7
	Stedv	7.2	7.5	0.0	6.9			
	Cov	0.0	0.0	0.0	0.0			

Figure 5-8 shows the viscosity measurement after RTFO aging, when tested at 50 rpm. At 105°C, the viscosity decreased by 8% when 2% silica fume was introduced to the control asphalt binder. In the presence of 4% silica fume, viscosity increased by 6%. At a temperature of 120°C, viscosity decreased by 6% when 2% of silica fume was introduced to the control asphalt binder,

while adding 4% and 8% silica fume increased the viscosity by 7% and 21%, respectively. At a temperature of 135°C (the standard testing temperature based on the ASTM D4402), a 5% decrease in viscosity was found when 2% of silica fume was introduced to the control asphalt binder. When 4% silica fume was added to the control binder, viscosity increased by 7%, while adding 8% silica fume increased the viscosity by 20%. At a high temperature of 150°C, adding 2% silica fume decreased viscosity by 1%, while adding 4% and 8% silica fume increased viscosity by 9% and 23%, respectively. The data is shown in Table 5-6.

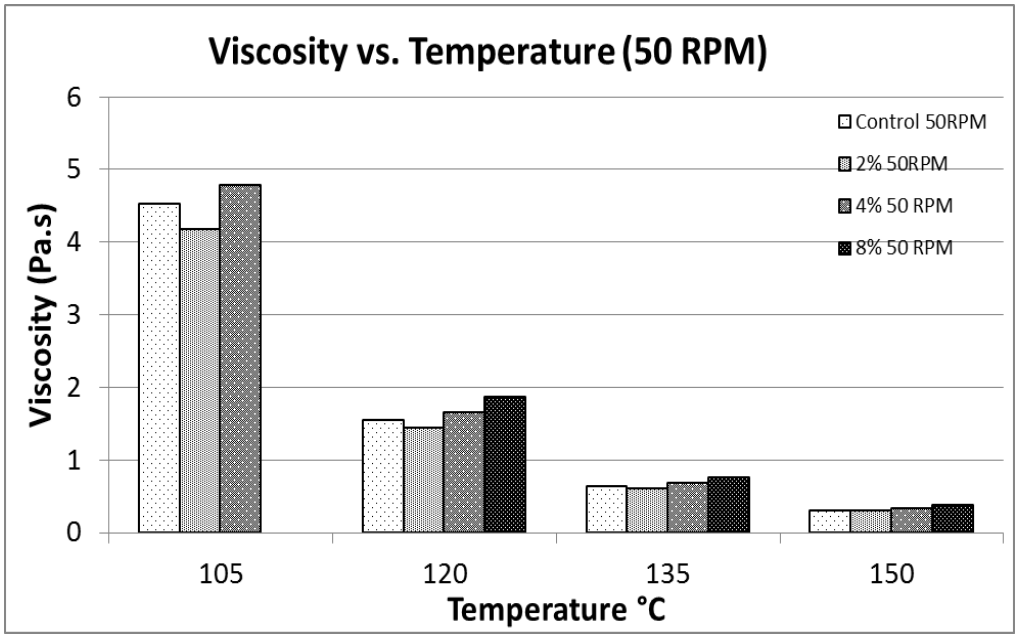

Figure 5-8. Viscosity vs. Temperature (°C) at 50 rpm (After Aging)

Table 5-6

Viscosity Measurements of Aged Samples at 50 rpm

Temp (°C)	Viscosity	Non-Modified PG 64-22	Silica fume Modified			Viscosity Variation		
			2%	4%	8%	2%	4%	8%
105	v1	4520.0	4175.0	4770.0	--	-7.6	5.5	--
	v2	4520.0	4170.0	4785.0	--	-7.7	5.9	--
	v3	4525.0	4175.0	4780.0	--	-7.7	5.6	--
	Average	4521.7	4173.3	4778.3	--	-7.7	5.7	--
	Stedv	2.9	2.9	7.6	--			
	Cov	0.0	0.0	0.0	--			
120	v1	1550.0	1445.0	1655.0	1865.0	-6.8	6.8	20.3
	v2	1540.0	1445.0	1655.0	1865.0	-6.2	7.5	21.1
	v3	1540.0	1445.0	1650.0	1860.0	-6.2	7.1	20.8
	Average	1543.3	1445.0	1653.3	1863.3	-6.4	7.1	20.7
	Stedv	5.8	0.0	2.9	2.9			
	Cov	0.0	0.0	0.0	0.0			
135	v1	640.0	610.0	685.0	765.0	-4.7	7.0	19.5
	v2	635.0	605.0	685.0	770.0	-4.7	7.9	21.3
	v3	640.0	605.0	685.0	760.0	-5.5	7.0	18.8
	Average	638.3	606.7	685.0	765.0	-5.0	7.3	19.8
	Stedv	2.9	2.9	0.0	5.0			
	Cov	0.0	0.0	0.0	0.0			
150	v1	305.0	300.0	330.0	375.0	-1.6	8.2	23.0
	v2	305.0	305.0	335.0	375.0	0.0	9.8	23.0
	v3	305.0	300.0	330.0	375.0	-1.6	8.2	23.0
	Average	305.0	301.7	331.7	375.0	-1.1	8.7	23.0
	Stedv	0.0	2.9	2.9	0.0			
	Cov	0.0	0.0	0.0	0.0			

5.4 Viscosity Aging Index

The viscosity aging index (VAI) is used to evaluate the extent of aging. It is calculated from the viscosity of the samples before and after short-term (RTFO) aging, according to the formula shown in Equation 5-1. The VAI indicates the extent of age hardening in terms of

viscosity (Zhang et al., 2012). The values of VAI for modified and non-modified specimens at 10 rpm are shown in Figure 5-9.

$$\text{VAI} = \frac{\text{Aged viscosity value} - \text{Unaged viscosity value}}{\text{Unaged viscosity value}} \qquad \text{Equation 5-1}$$

As can be seen in Figure 5-9, the VAI values for modified binders are overall significantly lower than those of control binders. At 10 rpm, introduction of 2% silica fume decreased the VAI by 23%. The 4% silica-fume-modified binder decreased the VAI by 53%, while 8% silica fume decreased the VAI by 47%. Thus, the 4% silica-fume-modified binder reflected the greatest decrease in the VAI.

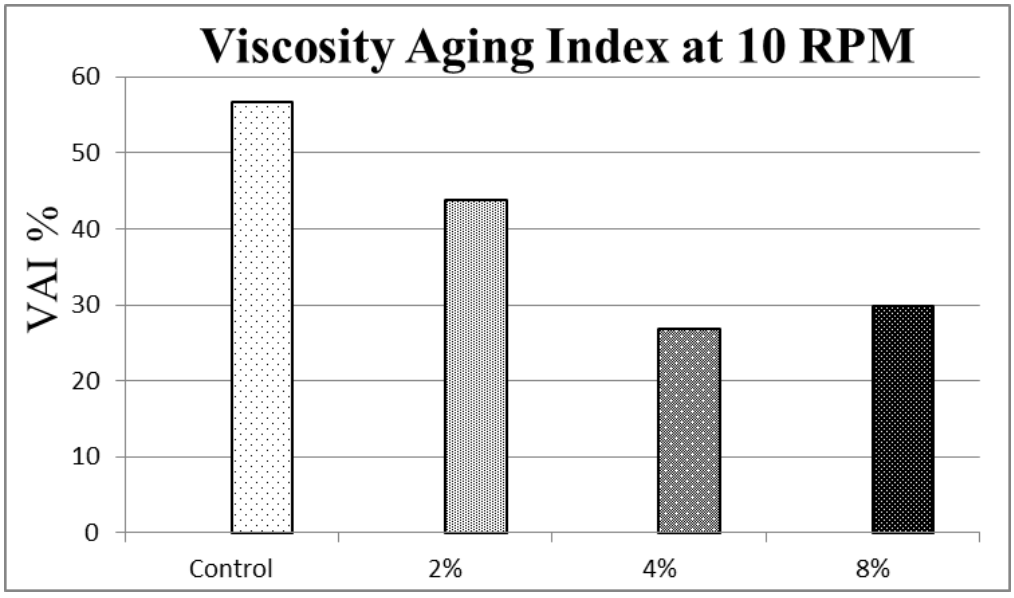

Figure 5-9. Viscosity Aging Index of Binders After Short-term Aging at 10 rpm

As can be seen in Figure 5-10, the VAI values at 20 rpm for silica-fume-modified binders are overall significantly lower than those of control binders. The VIA decreased by 47% when 2% silica fume was introduced to the control asphalt binder. With the addition of 4% silica fume, the VAI decreased by 50%. In the presence of 8% silica fume, the VAI decreased by 47%. So at 20 rpm, the 4% silica fume sample had the lowest VAI value, 30.51.

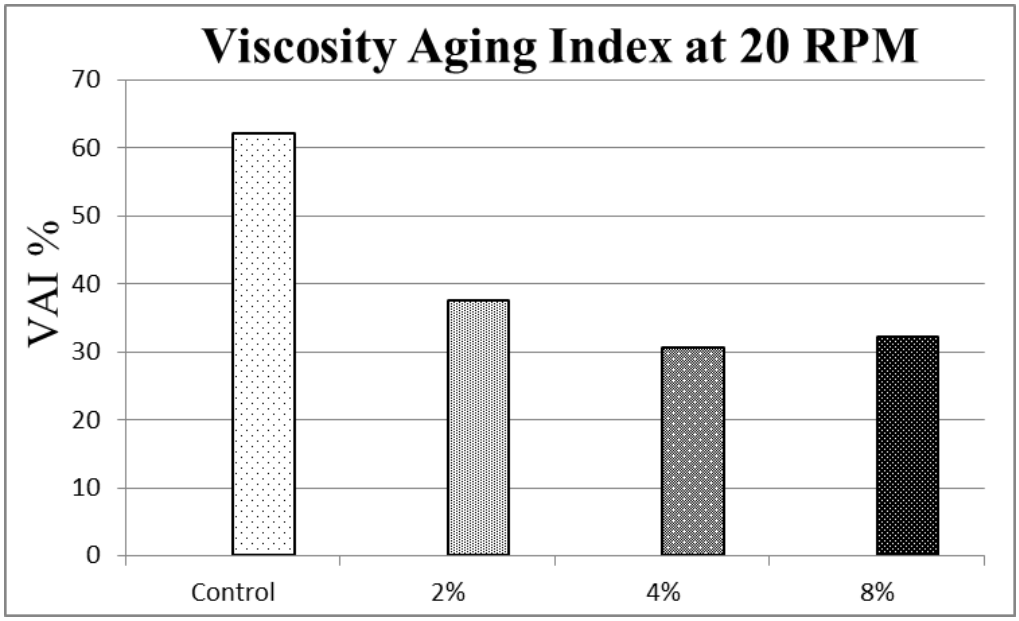

Figure 5-10. Viscosity Aging Index of Binders After Short-term Aging at 20 rpm

Figure 5-11 shows the VAI values for control binder and modified binders at 50 rpm. When 2% silica fume was introduced to control asphalt binder, the VIA decreased by 48%. A similar decrease was found with the addition of 4% silica fume. In the presence of 8% silica fume, the VAI decreased by 53% to the lowest VAI at 50 rpm.

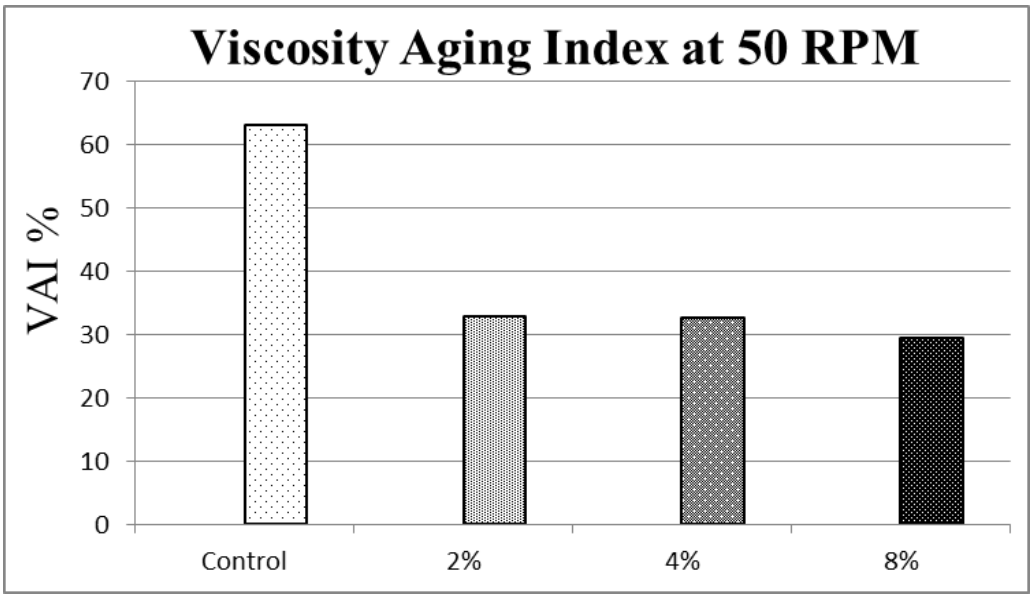

Figure 5-11. Viscosity Aging Index of Binders After Short-term Aging at 50 rpm

5.5 Shear Susceptibility

Shear Susceptibility (SS) is defined by Equation 5-2. Previous studies showed that binder with relatively small shear susceptibility (low gains in viscosity relative to the increase in shear rate) results in better overall pavement performance (Roberts et al., 1996).

$$\boldsymbol{SS} = \frac{\boldsymbol{log\ (Viscosity)}}{\boldsymbol{log\ (Shear\ Rate)}} \qquad \text{Equation 5-2}$$

The shear susceptibility at 120°C is indicated in Figure 5-12. As can be seen in Figure 5-12, the slope was found to be 0.0748 for the control asphalt. The slope reduced to 0.0315, 0.0588, and 0.0476 when 2%, 4%, and 8% silica fume was introduced, respectively. The shear susceptibility was reduced by 58%, 21%, and 36% for the addition of 2%, 4%, and 8% silica fume, respectively.

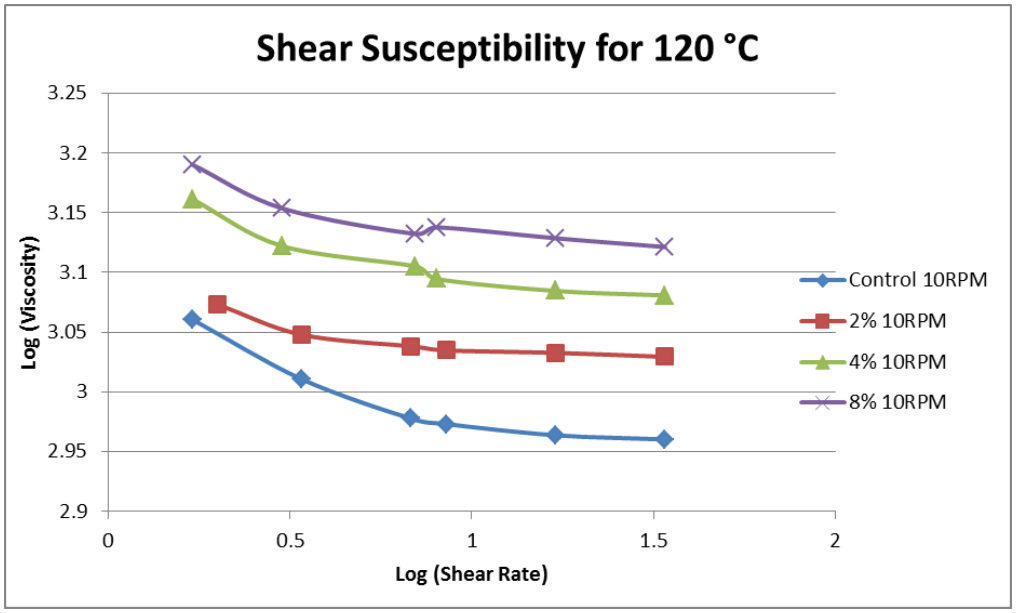

Figure 5-12. Shear Susceptibility for 120°C

5.6 Temperature Susceptibility

Temperature susceptibility is a measurement of a ratio of asphalt binder viscosity change to temperature change (Claudy and Martin, 1998). Temperature susceptibility was calculated using Equation 5-3 (Rasmussen, 2002). The VTS is proportional to the temperature susceptibility of the asphalt binder.

$$VTS = \frac{[\log\log(\eta T2) - \log\log(\eta T1)]}{\log(T2) - \log(T1)} \qquad \text{Equation 5-3}$$

Where T1 and T2 are the temperatures (°C)

ηT_1 and ηT_2 are the viscosities of the binder at the same points (cp)

Figure 5-13 plots the ratio of log log viscosity versus the temperature at a speed of 10 rpm. The slope was found to be 0.0524 for the control asphalt. The slope decreased to 0.0534, 0.0492, and 0.0489 when 2%, 4%, and 8% silica fume was introduced, respectively.

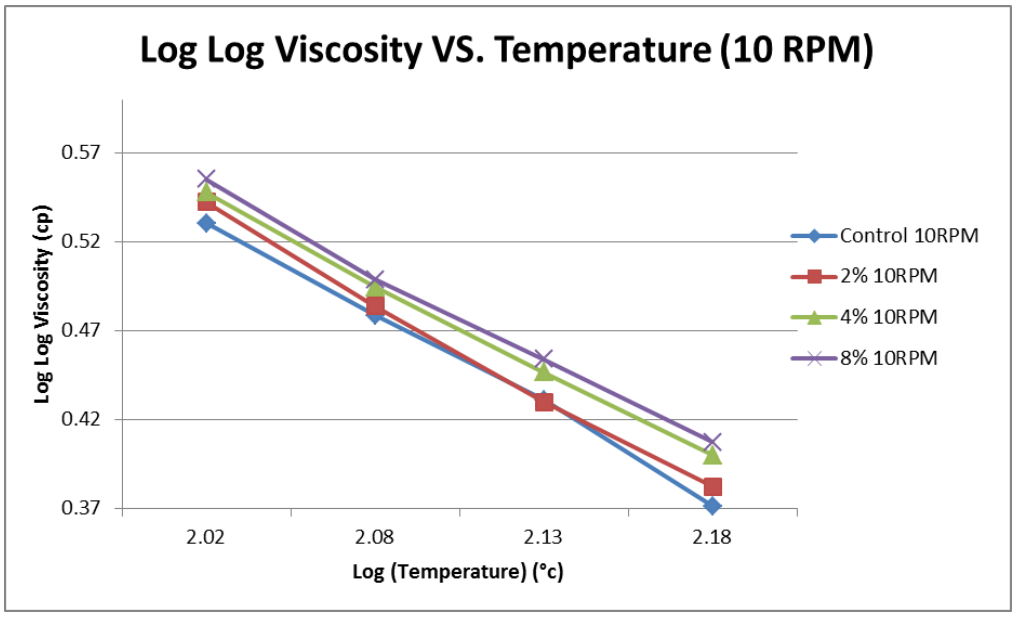

Figure 5-13. Temperature Susceptibility at 10 rpm

Figure 5-14 shows the ratio of log log viscosity versus the temperature at a speed of 50 rpm. In this case, the slope of the control was 0.0545, and it was reduced to 0.0525 when 8% silica fume was introduced.

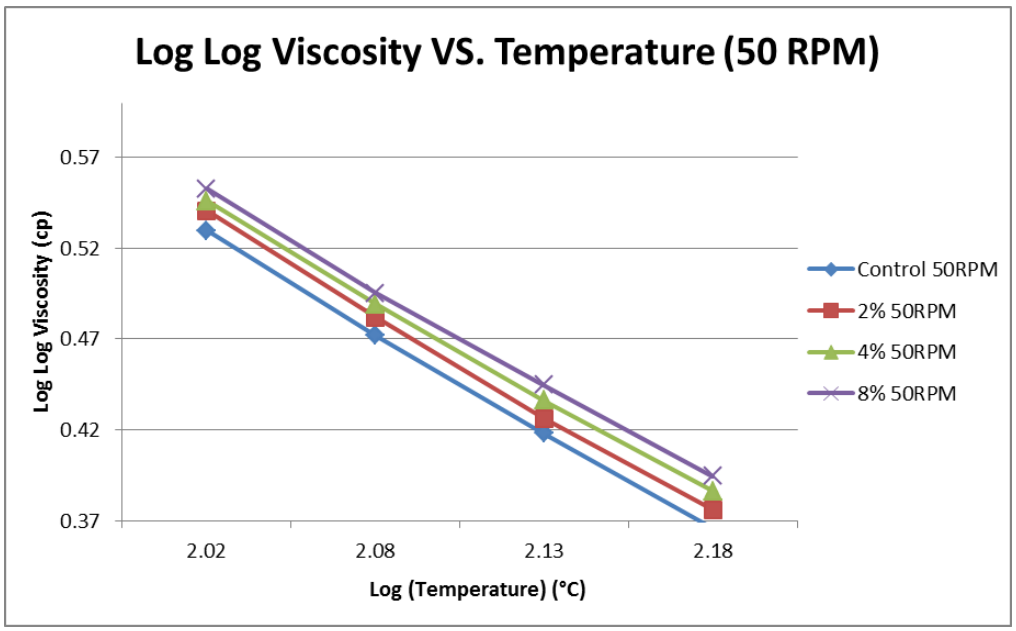

Figure 5-14. Temperature Susceptibility at 50 rpm

5.7 X-ray Diffraction

Data was collected between the angles of 4 and 60 °2 theta for a two hour period for each sample. All samples were tested on both incident and receiving sides. Test results were used to determine the crystallography of the mixtures being tested in this study. In fact, silica fume is amorphous. Therefore, diffraction peaks should not occur in these samples. Figure 5-15 shows silica fume samples at different percentages; no major changes were noticed due to inclusion of silica fume.

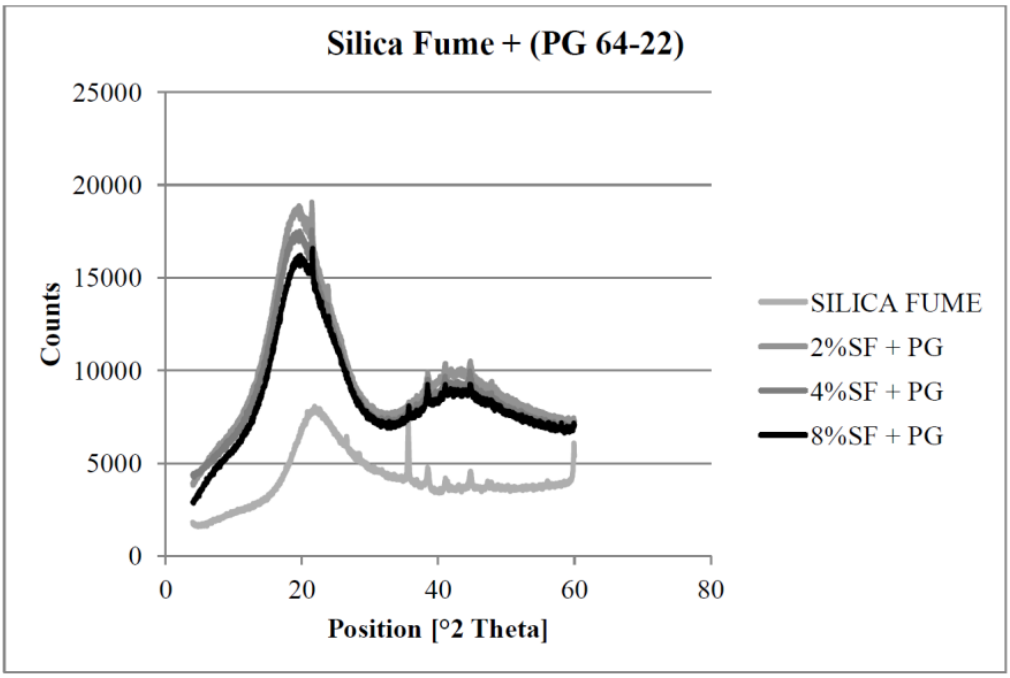

Figure 5-15. XRD Results of Silica Fume Blended with PG 64-22

5.8 Fourier Transform Infrared Spectroscopy

Silica fume is an amorphous polymorph of silicon dioxide, silica. Silica fume is a byproduct in the carbothermic reduction of high-quality quartz with carbonaceous materials. In Figure 5-16, the observed peaks do not correlate with the peaks of silicon, silicon dioxide, calcium oxide or aluminum oxide. The peak that occurs at 1639.22 cm-1 is related to a C-H bond for Alkanes. The peak that occurs at 1375.02 cm-1 refers to a C-H bond for Alkanes. The peak that occurs at 1107 cm-1 is related to a C-O bond. See Table 5-7.

Table 5-7

Description of IR absorptions (TutorVista, 2013)

Bond	Compound Type	Frequency Range, cm-1
C-H	Alkanes	2960-2850 (s) stretch
	CH; Umbrella Deformation	1470-1350 (v) scissoring and bending
		1380 (m-w) - Doublet - isopropyl, t-butyl
C-H	Alkanes	3080-3020 (m) stretch
		1000-675 (s) bend
C-H	Aromatic Rings	3100-3000 (m) stretch
	Phenyl Ring Substitution Bands	870-675 (s) bend
	Phenyl Ring Substitution Overtones	2000-1600 (w) - fingerprint region
C-H	Alkanes	3333-3267 (s) stretch
		700-610 (b) bend
C=C	Alkenes	1680-1640 (m,w) stretch
C°C	Alkynes	2260-2100 (w,sh) stretch
C=C	Aromatic Rings	1600, 1500 (w) stretch
C-O	Alcohols, Ethers, Caroxylic acids, Esters	1260-1000 (s) stretch
C=O	Aldehydes, Ketones, Carboxylic acids, Esters	1760-1670 (s) stretch
O-H	Monomeric -- Alcohols, Phenol	3640-3160 (s,br) stretch
	Hydrogen-bonded -- Alcohols, Phenols	3600-3200 (b) stretch
	Carboxylic acids	3000-2500 (b) stretch
N-H	Amines	3500-3300 (m) stretch
		1650-1580 (m) bend
C-N	Amines	1340-1020 (m) bend
C°N	Nitriles	2260-2220 (v) stretch
NO2	Nitro Compounds	1660-1500 (s) asymmetrical stretch
		1390-1260 (s) symmetrical stretch

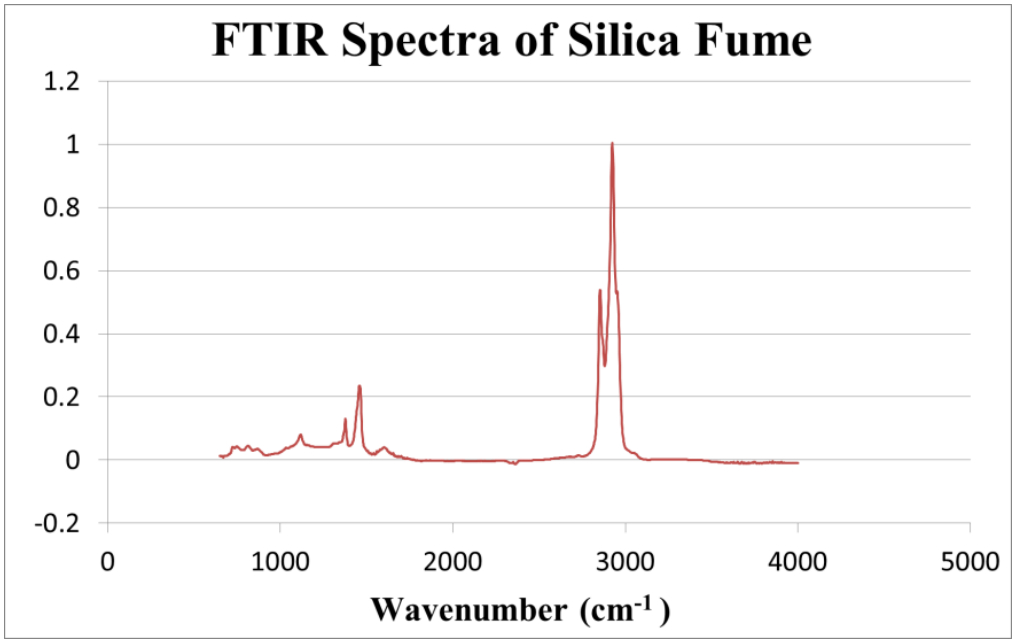

Figure 5-16. FTIR Spectra for 2% Silica Fume with PG at Room Temperature

CHAPTER 6

Discussion and Conclusions

6.1 Discussion

In this study, four laboratory tests were used: the Marshall test, the Rotational Viscosity (RV) test, the X-ray Diffraction (XRD) test, and the Fourier Transform Infrared Spectroscopy (FTIR) test. These tests were conducted at the Civil Engineering Laboratory at North Carolina A&T State University and at the Centre for Material Science and Engineering at Massachusetts Institute of Technology. Samples were prepared with different percentages of silica fume mixed with asphalt binder to identify the effects of adding silica fume to the asphalt binder.

The Marshall test was conducted to determine the stability and flow. Three different percentages of silica fume were added to a control asphalt binder AC 60-70. It was shown that adding silica fume can reduce the loss of stability, indicating that the silica fume particles can help improve the mixture stability while enhancing the workability.

The (RV) test was used to measure viscosity based on the rate of deformation due to an applied shear stress. 2%, 4%, and 8% samples were each tested three times. Temperature was set at the target temperature for different shear rates of 5, 10, 20, 25, 50, and 75 RPM. Data was collected for all six shear rates at temperatures of 105°C, 120°C, 135°C, and 150°C. The average of the three measurements was used to represent the viscosity of the sample at a specified temperature and shear rate. The collected data were then used to calculate the temperature susceptibility and shear susceptibility of each modified sample. It was shown that the viscosity increased with the addition of silica fume to the control asphalt binder (PG 64-22). Moreover, it was found that the 8% silica fume mixed with PG 64-22 has the lowest temperature susceptibility, followed by the 4% silica fume mixture.

The XRD test was used to determine the crystalline structure of silica fume added to PG 64-22. The sample was tested for two hours. Crystalline structure causes the incident ray to diffract in various directions. The angles and intensities of the diffracted rays were measured. Consequently, the density of the electrons within the crystal was clearly shown. The incident ray angle range was 4 – 60 degrees. Using a computer program, the peaks formed based on the crystalline structure of each sample were then analyzed, and the layer spacing was calculated. The results for the silica fume samples indicated that adding silica fume had little to no impact on the layer spacing, due to the non-crystalline form of silica fume.

The FTIR test was used to determine the compatibility of the silica fume with the asphalt binder. This test showed the formation of chemical bonds between silica fume and asphalt binder. The results of this test were dependent upon the shear rate (rate at which a sample was mixed) and compatibility of the asphalt binder used (PG 64-22). It showed the chemical components of silica fume associated with the description of IR absorptions table.

6.2 Conclusions

To reduce the oxidation rate of asphalt binder, silica fume was added to the base asphalt binder PG 64-22 at various percentages. The effectiveness of silica fume in reducing asphalt oxidation aging was evaluated experimentally. Four laboratory tests were conducted: the Marshall test, the X-ray Diffraction (XRD) test, the Fourier Transform Infrared Spectroscopy (FTIR) test, and the Rotational Viscosity (RV) test. Marshall tests were conducted to determine the stability and flow. It was shown that adding silica fume reduces loss of stability. The XRD and FTIR tests were used to study the crystalline structure of specimens and their chemical compositions. Study of viscosity results showed that significant increases in viscosity can be obtained by addition of silica fume to the control asphalt binder. Analysis of the experiment

results further showed that introduction of silica fume in asphalt binder can significantly reduce its oxidative aging in addition to enhancing stability and flow. The improvement was more noticeable at higher percentages of silica fume, up to 4%. However, above 4%, silica fume appeared to negatively affect the aging index, as measured by a higher aging index at 8% silica fume. The results of this research are expected to promote pavement service life by reducing oxidative aging while enhancing pavement sustainability and facilitating use of an industrial waste, silica fume.

It was found that 4% silica-fume-modified binder reduced oxidative aging by 50%, with a relatively low viscosity aging index (VAI) of 30.51. This is in line with the findings of prior research, which showed that introduction of 4% nano-silica could reduce oxidative aging by 29% (Onochie, 2013). It should be noted that silica fume was even more effective than nano-silica when the same percentages were used, and silica fume is currently considered an industrial waste and is frequently available at relatively low cost. Considering that the surface area of nano-silica is much higher than that of silica fume, nano-silica could be expected to be more effective in interacting with asphalt binder. However, the better aging performance of silica fume relative to nano-silica that was observed in this study could be attributed to a reduction in the agglomeration typically observed for nano-silica; agglomeration has been recognized as a problem in dealing with nano-silica. Therefore, the reduced agglomeration in silica fume could be linked to its improved oxidative aging performance.

6.3 Future Research

Further research is needed to specify the interaction mechanisms between silica fume and asphalt molecules. In addition, the optimum percentages of each additive should be determined in order to maximize the resulting improvement in asphalt binder aging resistance. Thus, it is

recommended that the molecular interactions between silica fume and asphalt binder be studied to provide in-depth understanding of the underlying mechanisms controlling the rheological properties of silica-fume-modified asphalt.

References

ASTM International. (2013). Products and Services, Standards and Publications. Accessed on May 21, 2014, from: www.astm.org.

Association of Asphalt Paving Technologists Technical Sessions. (1985). Marshall Procedures for Design and Quality Control of Asphalt Mixtures. *Asphalt Paving Technology*, *54*, 265-284.

Amirkhanian, A., Xiao, F., & Amirkanian, S. (2011). Evaluation of High Temperature Rheological Characteristics of Asphalt Binder with Carbon Nano Particles. *Journal of Testing and Evaluation*, *39* (4), 583-591.

Claudy, P., & Martin, D. (1998). Thermal Behavior of Asphalt Cements. *Thermochemical Act., 324*, 203-213.

Dutrow, B., & Clark, C. (2013). X-ray Powder Diffraction (XRD). The Science Education Resource Center at Carleton College. Accessed on June 19, 2014, from: http://serc.carleton.edu/research_education/geochemsheets/techniques/XRD.html

Federal Highway Administration (2012). Silica Fume. Washington, DC: United States Department of Transportation. Accessed on August 19, 2013, from: http://www.fhwa.dot.gov/infrastructure/materialsgrp/silica.htm

Gapinski, G., & Scanlon, J. (2011). Silica Fume. Norchem, Inc. Accessed on September 04, 2013, from: http://www.norchem.com/pdf/technical-papers-articles-gapinksi-scanlon.pdf.

Haipeng, J., Huang, Z., Chen, K., Li, W., Gao, Y., Fang, M., Liu, Y., & Wu, X. (2014). Synthesis of Si3N4 powder with tunable α/β-Si3N4 content from waste silica fume using carbothermal reduction nitridation. *Powder Technology*, *252*, 51–55.

Hosseini, S., Madaeni, S., & Khodabakhshi, A. (2010). Preparation and Characterization of ABS/HIPS Heterogeneous Anion Exchange Membrane Filled with Activated Carbon. *J. Appl. Polym. Sci., 118*, 3371–3383.

Huang, S., Glaser, R., & Turner, F. (2012). Impact of Water on Asphalt Aging: Chemical Aging Kinetic Study. *Transportation Research Record, 2293*, 63-72.

Khayat, K., Vachon, M., & Lanctot, M. (1997). Use of Blended Silica Fume Cement in Commercial Concrete Mixtures. *Materials Journal, 94* (3), 183-192.

Langan, B., Weng, K., & Ward, M.A. (2002). Effect of Silica Fume and Fly Ash on Heat of Hydration of Portland Cement. *Cement and Concrete Research, 32*, 1045-1051.

Lavin, P. (2003). Asphalt Pavements: A Practical Guide to Design, Production and Maintenance for Engineers and Architects. London: Spon Press.

Lee, L., Zeng, C., Cao, X., Han, X., Shen, J., & Xu, G. (2005). Polymer Nanocomposite. *Composites Science and Technology, 65*, 2344-2363.

Lu, X., & Isacsson, U. (2002). Effect of ageing on bitumen chemistry and rheology. *Construction and Building Materials, 16* (1), 15-22.

Mikoc, M., & Markovic, D. (2010). Influence Of Slag, Fly Ash and Silica Fume on the Mechanical and Physical Properties of Asphalt. *Technical Gazette, 17*(4), 505-514.

Onochie, A., Fini, E., Yang, X., Mills-Beale, J., & You, Z. (2013). Rheological Characterization of Nano-particle based Bio-modified Binder. Transportation Research Board 92nd annual Meeting. Washington, DC: Transportation Research Board. Available from: http://pubsindex.trb.org/view/2013/C/1242863

Parviz, A. (2011). Nano Materials in Asphalt and Tar. *Australian Journal of Basic and Applied Sciences, 5*(12), 3270-3273.

Rasmussen, R., Robert, L., & George, C. (2002). Method to Predict Temperature Susceptibility of an Asphalt Binder. *Journal of Materials in Civil Engineering, 14*, 246-252.

Roberts F., Kandhal, P., Brown, E., Lee, D., & Kennedy, T. (1996). Hot Mix Asphalt Materials, Mixture Design & Construction. Lanham, MD: National Asphalt Pavement Association.

Silica Fume Association. (2005). Silica Fume User's Manual. Accessed July 14, 2014 from: http://www.silicafume.org/concrete-manual.html

Specialists in Business Information (SBI). (2009). Report on Asphalt Manufacturing in the U.S. Accessed on April 30, 2014, from: http://www.sbireports.com/about/release.asp?id=1475

U.S. Oil & Refining Co. (n.d.). Paving Grade Asphalt, PG64-22. Accessed on May 27, 2014 from: http://www.usor.com/files/pdf/6/PG64-22.pdf.

Yildirim, Y. (2007). Polymer modified asphalt binders. *Construction and Building Materials, 21*, 66-72.

You, Z., Beale, J., Foley, J., Roy, S., Odegard, G., Dai, Q., & Wei Goh, S. (2011). Nanoclay-modified asphalt materials: Preparation and characterization. *Journal of Construction and Building Materials, 25*, 1072-1078.

Yu, J., Wang, X., Hu, L., & Tao, Y. (2010). Effect of Various Organomodified Montmorillonite/Bitumen Nanocomposites. *Journal of Materials in Civil Engineering, 22* (8), 788-793.

Zhang, H., Yu, J, & Wu, S. (2012). Effect of montmorillonite organic modification on ultraviolet aging properties of SBS modified bitumen. *Construction Building Materials, 27*, 553-559.